Magmatism, migrating topography, and the transition from Sevier shortening to Basin and Range extension, western USA

Jens-Erik Lund Snee[1] and Elizabeth L. Miller[2]

[1]U.S. Geological Survey Geosciences and Environmental Change Science Center, P.O. Box 25046, MS 980, Denver, CO 80225

[2]Stanford University Department of Geological Sciences, 450 Serra Mall Bld. 320, Room 118, Stanford, CA 94305

ABSTRACT

The paleogeographic evolution of the western USA Great Basin from the Late Cretaceous to the Cenozoic is critical to understanding how the Cordillera at this latitude transitioned from Mesozoic shortening to Cenozoic extension. According to a widely applied model, Cenozoic extension was driven by collapse of elevated crust supported by crustal thicknesses that were potentially double the present ~30–35 km. This model is difficult to reconcile with more recent estimates of moderate regional extension (≤50%) and the discovery that most high-angle, basin–range faults slipped rapidly ca. 17 Ma, tens of millions of years after crustal thickening occurred. Here we integrate new and existing geochronology and geologic mapping in the Elko area of northeast Nevada, one of the few places in the Great Basin with substantial exposures of Paleogene strata. We improve age control for strata that have been targeted for studies of regional paleoelevation and paleoclimate across this critical time span. In addition, a regional compilation of the ages of material within a network of middle Cenozoic paleodrainages developed across the Great Basin shows that the age of basal paleovalley fill decreases southward roughly synchronous with voluminous ignimbrite flareup volcanism that swept south across the region ca. 45–20 Ma. Integrating these datasets with the regional record of faulting, sedimentation, erosion, and magmatism, we suggest that volcanism was accompanied by an elevation increase that disrupted drainage systems and shifted the continental divide east into central Nevada from its Late Cretaceous location along the Sierra Nevada arc. The north–south Eocene–Oligocene drainage divide defined by mapping of paleovalleys may thus have evolved as a dynamic feature that propagated southward with magmatism. Despite some local faulting, the northern Great Basin became a vast, elevated volcanic tableland that persisted until dissection by Basin and

Range faulting that began ca. 21–17 Ma. Based on this more detailed geologic framework, it is unlikely that Basin and Range extension was driven by Cretaceous crustal overthickening; rather, pre-existing crustal structure was just one of several factors that that led to Basin and Range faulting after ca. 17 Ma—in addition to thermal weakening of the crust associated with Cenozoic magmatism, thermally supported elevation, and changing boundary conditions. Because these causal factors evolved long after crustal thickening ended, during final removal and fragmentation of the shallowly subducting Farallon slab, they are compatible with normal (~45–50 km) thickness crust beneath the Great Basin prior to extension and do not require development of a strongly elevated, Altiplano-like region during Mesozoic shortening.

INTRODUCTION

The switch from Mesozoic shortening to Cenozoic extension in the western USA Cordillera was a fundamental tectonic transition with implications for orogenic systems worldwide, but its causes remain hotly debated and poorly understood. The many models focusing on this time interval reveal disagreements regarding these basic questions: What was the pre-extensional crustal structure, crustal thickness, and resulting topography across the west? What was the causal mechanism for initiation of continental extension? What was the detailed timing of important tectonic events across this time span and how do those events factor into our understanding of causal mechanisms for the switch from shortening to extension?

The prevailing view argues that Mesozoic crustal thickening in the Sevier fold and thrust belt produced a high plateau (the "*Nevadaplano*") across the region of the present-day Great Basin (Fig. 1) (DeCelles, 2004). Although the concept of the *Nevadaplano* is widely accepted, there is little agreement regarding the timing and cause of plateau uplift (cf. Parsons et al., 1994; Mix et al., 2011; Cassel et al., 2018), its peak elevation (cf. Chase et al., 1998; Wolfe et al., 1998; Best et al., 2009; Cassel et al., 2012), whether or not "rugged topography" may have been present on the plateau (cf. Chamberlain et al., 2007; Henry et al., 2012; Bahadori et al., 2018), and the causes and timing of its inferred "collapse" (cf. Sonder et al., 1987; McQuarrie and Chase, 2000; Colgan and Henry, 2009; Wells et al., 2012; Lee et al., 2017).

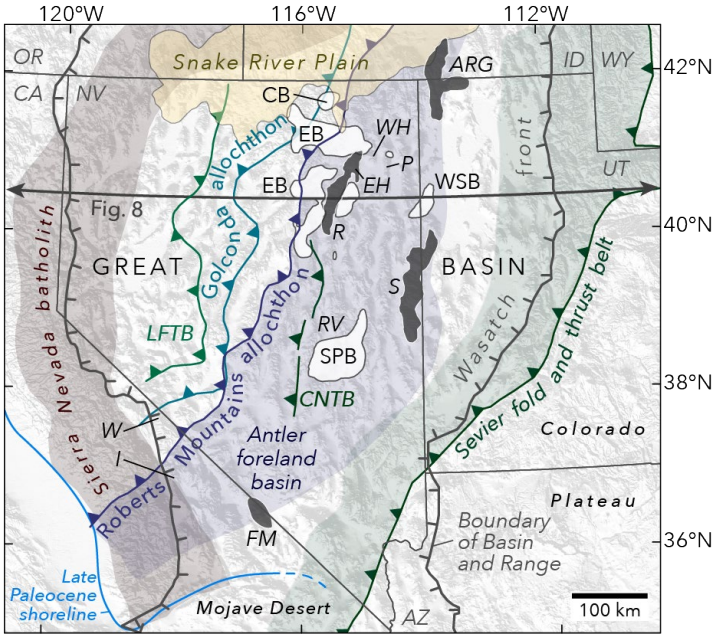

Figure 1. The Great Basin, including the northern and central Basin and Range province (BRP), western USA. The Mesozoic Sierra Nevada batholith is after Van Buer and Miller (2010). Paleogene basins are from Haynes (2003) and Smith et al. (2017). The approximate late Paleocene ocean shoreline is after Reid (1988) and Lechler and Niemi (2011). Luning-Fencemaker thrust belt (LFTB) locations are from Best et al. (2009). Locations of the Golconda and Roberts Mountains allochthons, Central Nevada thrust belt, and Sevier belt are from DeCelles (2004). The BRP boundary is from Dickinson (2013). ARG—Albion–Raft River–Grouse Creek Mountains; CB—Copper Basin; CNTB—Central Nevada thrust belt; EB—Elko Basin; EH—East Humboldt Range; FM—Funeral Mountains; I—Inyo Mountains; P—Pequop Mountains; R—Ruby Mountains; RV—Railroad Valley; S—Snake Range; SPB—Sheep Pass Basin, W—White Mountains; WH—Wood Hills; WSB—White Sage Basin.

Related to these broader questions are more detailed questions about the resulting topography across this region. Studies based on the pattern of Cenozoic ash-flow tuffs that filled paleovalleys (e.g., Best et al., 2013; Henry and John, 2013) indicate a ~north–south-oriented divide that passed down the middle of central Nevada (Fig. 2), slightly west of the mostly older, Eocene Elko Basin (e.g., Haynes, 2003; Lund Snee et al., 2016; Camilleri et al., 2017) and the mostly Late Cretaceous and Eocene Sheep Pass Basin (e.g., Druschke et al., 2009a, 2009b). However, the divide has also been inferred to lie along the axis of the Mesozoic Sierra Nevada arc during the Late Cretaceous (Van Buer et al., 2009; Sharman et al., 2015). When, why and how did this eastward shift of the divide occur? Was the shift related to the south-sweeping middle Cenozoic volcanism of the ignimbrite flareup in the retroarc region (Fig. 2) (e.g.,

Armstrong and Ward, 1991; Christiansen and Yeats, 1992)? How did volcanism and the addition of large volumes of magma and heat affect retroarc topography?

Here we integrate new and previously published geologic mapping and U-Pb detrital zircon geochronology from Late Cretaceous(?)–Neogene sedimentary and volcanic rocks of the Elko Basin of northeast Nevada, one of the only successions spanning large portions of the time between Cretaceous crustal thickening and Neogene Basin and Range extension (Figs. 1 and 2). We discuss the paleogeographic and tectonic significance of the stratigraphic succession and published stable isotope records in the Elko area in the context of others from throughout the region. We also compiled ages for the oldest volcanic or sedimentary material deposited in a network of east- and west-draining paleovalleys active across the Great Basin in middle Cenozoic time. Drawing upon all of this information, we present a revised view of the paleogeographic and tectonic evolution of the northern Great Basin from Late Cretaceous to Neogene time. Finally, we discuss the implications for estimates of crustal thickness and topography prior to Cenozoic extension, including impacts for the *Nevadaplano* model.

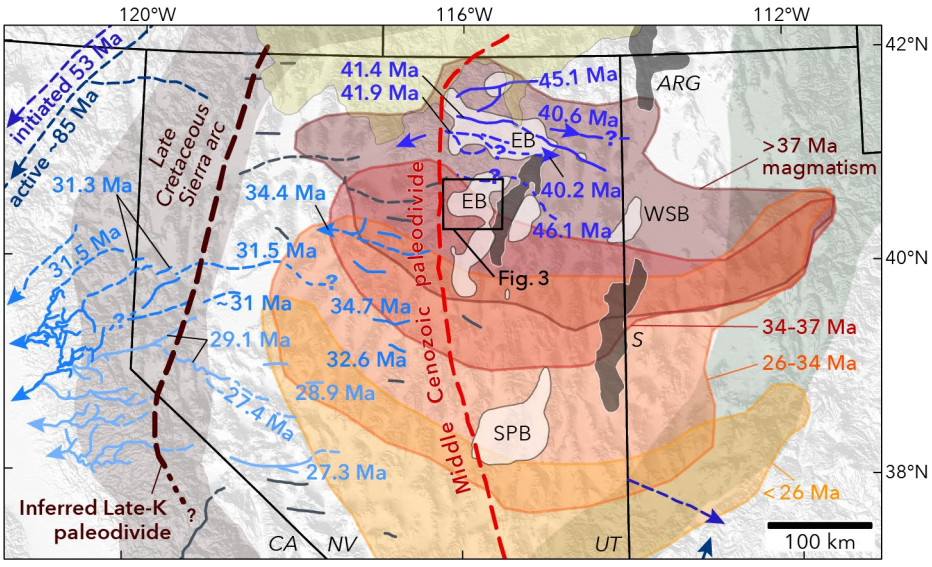

Figure 2. Late Cretaceous and Cenozoic volcanism and topography in the Great Basin, showing paleodrainages colored by the age of oldest reported material deposited within them, compiled from sources in the GSA Data Repository. Lighter blues represent younger paleodrainages, and gray indicates no age information. The approximate location of the Late Cretaceous paleodivide is inferred from Van Buer et al. (2009) and Sharman et al. (2015). The Cenozoic paleodivide is from Henry and John (2013) and represents the conventional view that the drainage divide was broadly static over Eocene–Oligocene time (and possibly earlier). Volcanic fields

are based on data from the North American Volcanic and Intrusive Rock Database (NAVDAT; http://ecp.iedadata.org). Other references and acronyms as in Fig. 1.

GEOLOGIC SETTING

Late Cretaceous and Cenozoic strata in northeast Nevada, in the area of the Eocene Elko Basin (Figs. 1–3), unconformably overlie a thick (~10 km) Neoproterozoic to Triassic section deposited along the passive margin of western North America (e.g., Willden and Kistler, 1979; Colgan et al., 2010), formed after Neoproterozoic and early Paleozoic rifting of the Rodinia supercontinent (e.g., Lund, 2008; Yonkee et al., 2014). West of the Elko area lie deep-marine rocks of the Roberts Mountains and Golconda allochthons (Fig. 1) that were respectively thrust across the continental margin in the earliest Mississippian and the Permian-Triassic (e.g., Stewart, 1980). These relations and the location of the initial $^{87}Sr/^{86}Sr = 0.706$ isopleth imply that western Nevada was underlain by oceanic crust and that the thick passive margin succession at the study area in northeast Nevada was underlain by thinned continental crust (Tosdal et al., 2000). East-dipping subduction beneath the Cordilleran margin initiated as early as the Early Triassic (e.g., Saleeby et al., 2008). The study area, which was in the retroarc region of the Sierra Nevada arc, experienced two episodes of shortening and metamorphism during periods of increased arc magmatism, one in the Middle to Late Jurassic ca. 170–155 Ma and the second in the Late Cretaceous ca. 120–70 Ma (e.g., Dallmeyer et al., 1986; Miller and Gans, 1989; Thorman et al., 1991; Smith et al., 1993; McGrew and Snee, 1994; Thorman and Peterson, 2003; Du Bray, 2007; Zuza et al., 2020). Cretaceous thrust faulting at the latitudes of northern and central Nevada was confined mostly to the Sevier fold and thrust belt to the east of the study area, with significantly less shortening represented by the Central Nevada thrust belt in central and southern Nevada (Fig. 1) (Taylor et al., 2000; Di Fiori et al., 2020).

Following Late Cretaceous subduction-related arc magmatism, volcanism initiated again as part of the middle Cenozoic ignimbrite flareup, characterized by widespread caldera-forming volcanism that migrated southward across the Great Basin, passing through northeast Nevada (Fig. 2) ca. 42–36 Ma (Brooks et al., 1995; Ressel and Henry, 2006; Ryskamp et al., 2008; Henry and John, 2013; Lund Snee et al., 2016). Although extension initiated locally as early as Eocene time in certain areas (e.g., Henry et al., 2011; Miller et al., 2012; Wells et al., 2012), recognition is growing that the primary extension that affected topography and supracrustal rocks across the

hinterland was an episode of rapid slip on high-angle normal faults that took place mostly during middle to late Miocene time and culminated in the present Basin and Range topography (Lund et al., 1993; Miller et al., 1999; Stockli et al., 2002; Henry, 2008; Colgan and Henry, 2009; Colgan et al., 2010; Colgan, 2013; Konstantinou and Miller, 2015; Lund Snee et al., 2016). This contribution presents new geochronologic and geological data obtained in the ancestral Elko Basin. We then examine the sedimentary record for the constraints it provides on the controversial and enigmatic history of the Late Cretaceous to the Miocene and, specifically, how the surface topography may have changed across this time span.

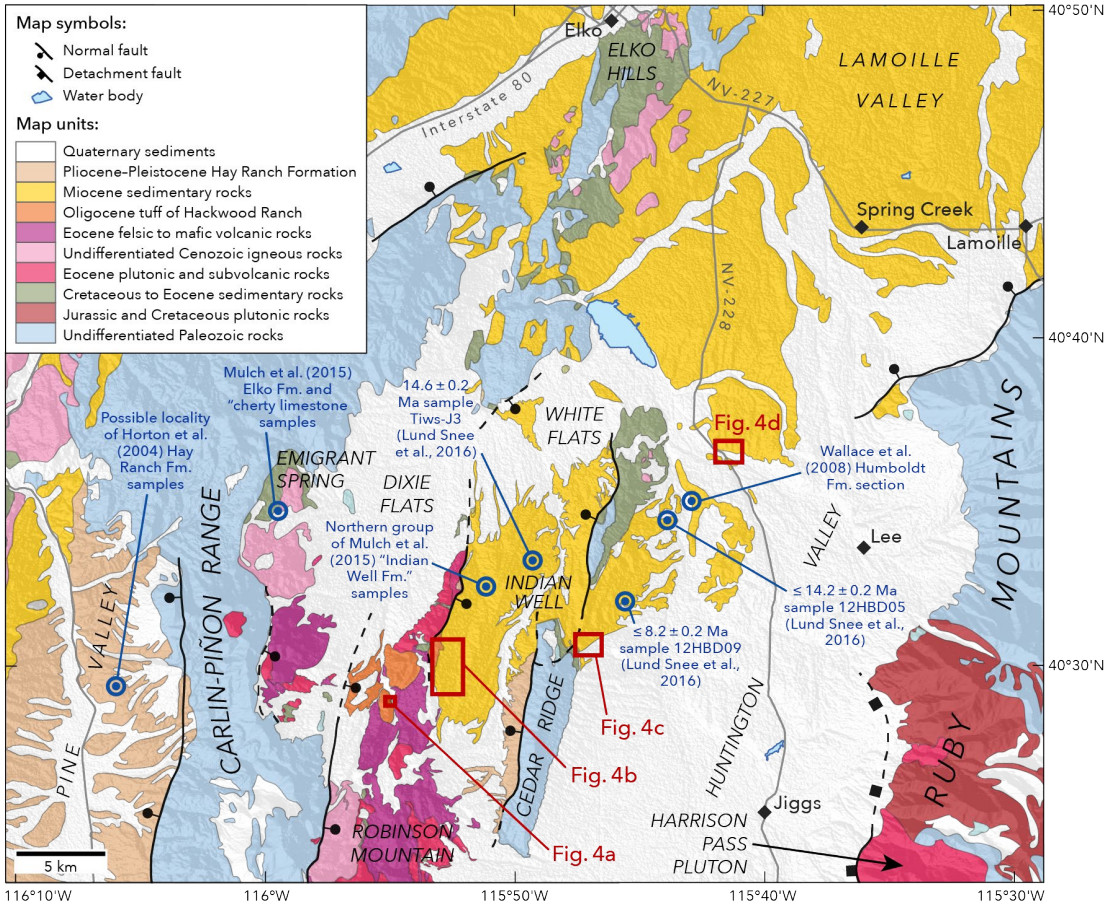

Figure 3. Geologic map of the ancestral Elko Basin region, northeast Nevada (location shown in Fig. 2). Unit boundaries and faults are from Crafford (2007), Colgan et al. (2010), Lund Snee et al. (2016), and this study. The Ruby-East Humboldt detachment fault is presently a shallowly dipping fault system that experienced both ductile and brittle deformation (e.g., Dokka et al., 1986).

METHODS

We mapped geologic units and tuffaceous beds, measured stratigraphic sections (Fig. 5), and collected samples for U-Pb detrital zircon geochronology in Oligocene and Miocene successions in Huntington Valley and the eastern Carlin-Piñon Range, northeast Nevada (Figs. 3 and 4), in and near the ancestral Elko Basin (Figs. 1 and 2). Our work refines geologic mapping by Smith and Howard (1977), Smith and Ketner (1978), Lund Snee (2013), Lund Snee and Miller (2015), and Lund Snee et al. (2016), who provided detailed descriptions of those rocks. The GSA Data Repository contains detailed analytical methods and it presents the results of seven additional U-Pb detrital zircon analyses to those by Lund Snee et al. (2016). Figure 5 shows the new and previous geochronology results within their *stratigraphic* framework.

Some of the same sections have previously been sampled for stable isotope analysis of calcite cements, limestone, and paleosols (Horton et al., 2004; Mix et al., 2011) and our work refines the age constraints and understanding of the depositional context for Neogene rocks within those sections. Figure 6 shows stable isotope data from prior studies placed in their revised *temporal* positions, with permissible depositional ages conservatively bounded by the full 2σ uncertainty ranges for the depositional age constraints (e.g., including the 2σ uncertainties for weighted mean ages). The Data Repository presents detailed methods for assigning age constraints and preferred depositional ages, and it includes tables containing lithologic details, sample localities, (maximum) depositional age information, and analytical data. Using these same methods, we used published geochronologic data to improve depositional age constraints for published stable isotope data that were obtained in older, Paleogene strata in the area (locations in Fig. 3), for which a number of contradictory depositional ages have been reported (cf. Horton et al., 2004; Mix et al., 2011; Chamberlain et al., 2012; Mulch et al., 2015; Smith et al., 2017). In most cases, the permissible age bounds were not given in those studies, and sample ages were reported as being absolute when in fact they were maximum depositional ages (MDAs).

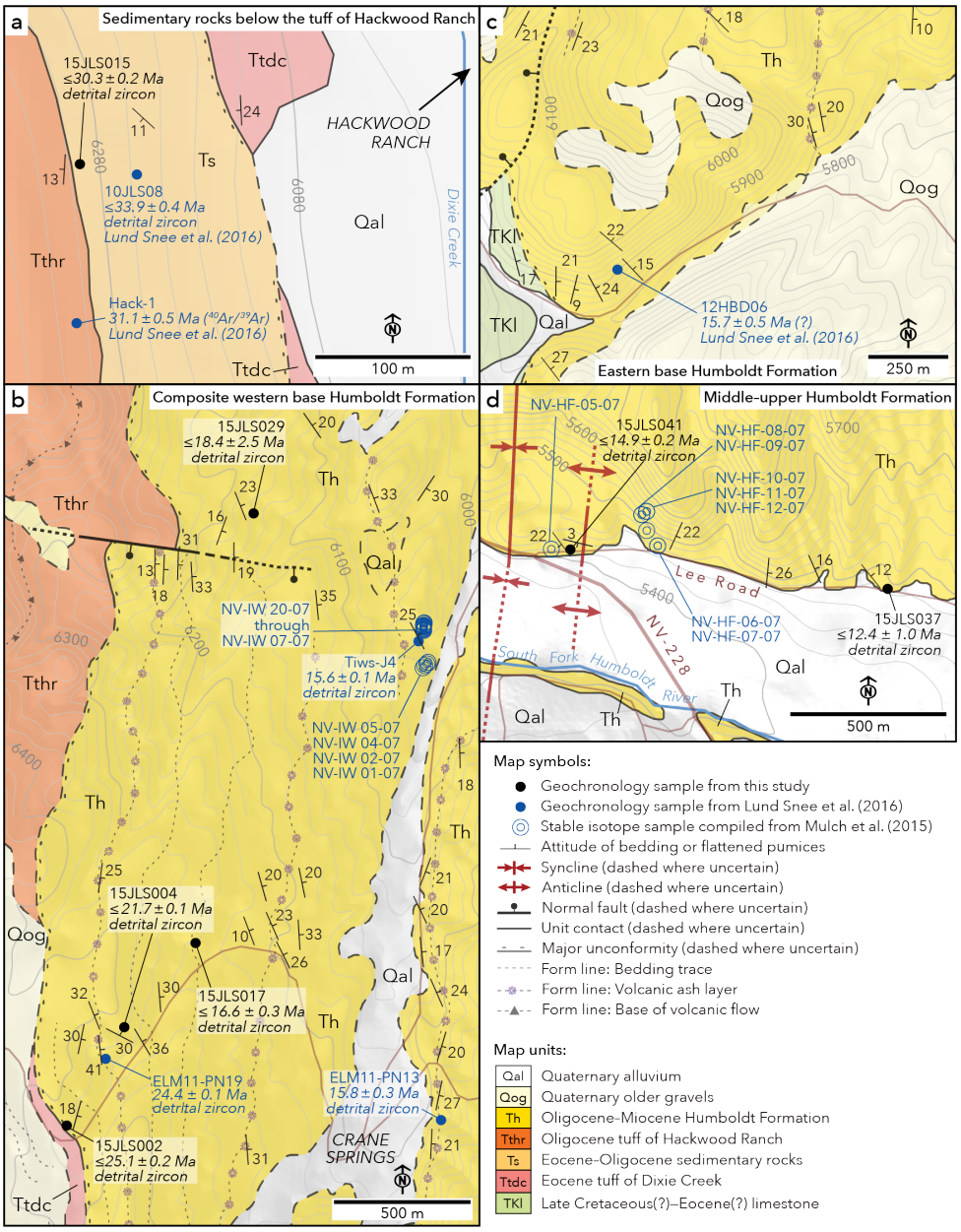

Figure 4. Geologic maps of areas sampled for this study. Unit boundaries and structures are from Smith and Howard (1977), Crafford (2007), Lund Snee and Miller (2015), Lund Snee et al. (2016), and this study. Maximum depositional ages are indicated with inequality symbols ("≤"), unlike for nearly absolute depositional ages from tuffaceous horizons.

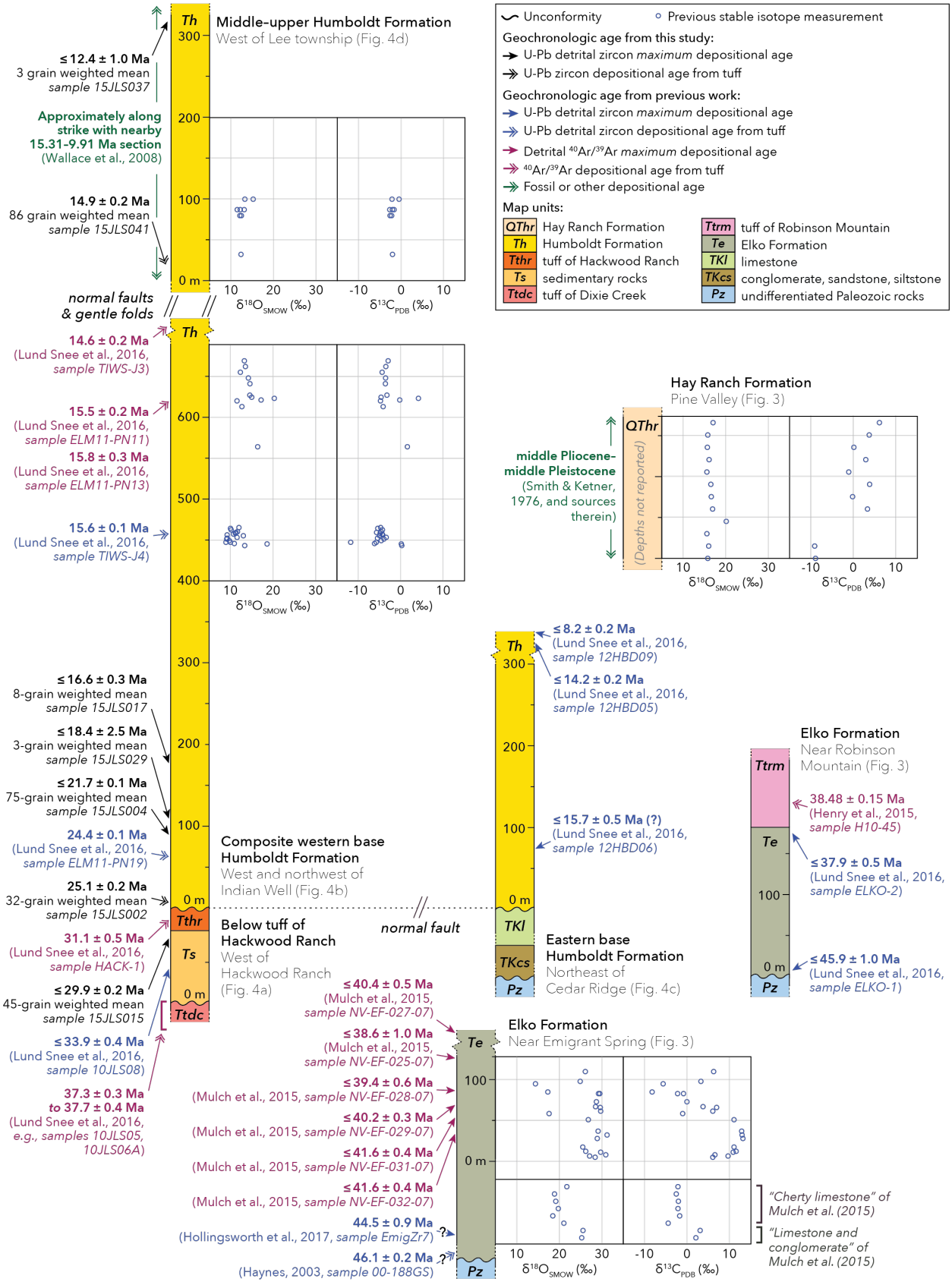
Unconformity
Previous stable isotope measurement
Geochronologic age from this study:
U-Pb detrital zircon maximum depositional age
U-Pb zircon depositional age from tuff
Geochronologic age from previous work:
U-Pb detrital zircon maximum depositional age
U-Pb detrital zircon depositional age from tuff
Detrital 40Ar/39Ar maximum depositional age
40Ar/39Ar depositional age from tuff
Fossil or other depositional age
Map units:
QThr Hay Ranch Formation
Th Humboldt Formation
Tthr tuff of Hackwood Ranch
Ts sedimentary rocks
Ttdc tuff of Dixie Creek
Ttrm tuff of Robinson Mountain
Te Elko Formation
TKl limestone
TKcs conglomerate, sandstone, siltstone
Pz undifferentiated Paleozoic rocks
Middle-upper Humboldt Formation
West of Lee township (Fig. 4d)
≤ 12.4 ± 1.0 Ma
3 grain weighted mean
sample 15JLS037
Approximately along strike with nearby 15.31–9.91 Ma section (Wallace et al., 2008)
14.9 ± 0.2 Ma
86 grain weighted mean
sample 15JLS041
normal faults & gentle folds
14.6 ± 0.2 Ma (Lund Snee et al., 2016, sample TIWS-J3)
15.5 ± 0.2 Ma (Lund Snee et al., 2016, sample ELM11-PN11)
15.8 ± 0.3 Ma (Lund Snee et al., 2016, sample ELM11-PN13)
15.6 ± 0.1 Ma (Lund Snee et al., 2016, sample TIWS-J4)
≤ 16.6 ± 0.3 Ma
8-grain weighted mean
sample 15JLS017
≤ 18.4 ± 2.5 Ma
3-grain weighted mean
sample 15JLS029
≤ 21.7 ± 0.1 Ma
75-grain weighted mean
sample 15JLS004
24.4 ± 0.1 Ma (Lund Snee et al., 2016, sample ELM11-PN19)
25.1 ± 0.2 Ma
32-grain weighted mean
sample 15JLS002
31.1 ± 0.5 Ma (Lund Snee et al., 2016, sample HACK-1)
≤ 29.9 ± 0.2 Ma
45-grain weighted mean
sample 15JLS015
≤ 33.9 ± 0.4 Ma (Lund Snee et al., 2016, sample 10JLS08)
37.3 ± 0.3 Ma to 37.7 ± 0.4 Ma (Lund Snee et al., 2016, e.g., samples 10JLS05, 10JLS06A)
Composite western base Humboldt Formation
West and northwest of Indian Well (Fig. 4b)
Below tuff of Hackwood Ranch
West of Hackwood Ranch (Fig. 4a)
normal fault
Hay Ranch Formation
Pine Valley (Fig. 3)
middle Pliocene–middle Pleistocene (Smith & Ketner, 1976, and sources therein)
(Depths not reported)
≤ 8.2 ± 0.2 Ma (Lund Snee et al., 2016, sample 12HBD09)
≤ 14.2 ± 0.2 Ma (Lund Snee et al., 2016, sample 12HBD05)
≤ 15.7 ± 0.5 Ma (?) (Lund Snee et al., 2016, sample 12HBD06)
Eastern base Humboldt Formation
Northeast of Cedar Ridge (Fig. 4c)
Elko Formation
Near Robinson Mountain (Fig. 3)
38.48 ± 0.15 Ma (Henry et al., 2015, sample H10-45)
≤ 37.9 ± 0.5 Ma (Lund Snee et al., 2016, sample ELKO-2)
≤ 45.9 ± 1.0 Ma (Lund Snee et al., 2016, sample ELKO-1)
≤ 40.4 ± 0.5 Ma (Mulch et al., 2015, sample NV-EF-027-07)
≤ 38.6 ± 1.0 Ma (Mulch et al., 2015, sample NV-EF-025-07)
≤ 39.4 ± 0.6 Ma (Mulch et al., 2015, sample NV-EF-028-07)
≤ 40.2 ± 0.3 Ma (Mulch et al., 2015, sample NV-EF-029-07)
≤ 41.6 ± 0.4 Ma (Mulch et al., 2015, sample NV-EF-031-07)
≤ 41.6 ± 0.4 Ma (Mulch et al., 2015, sample NV-EF-032-07)
44.5 ± 0.9 Ma (Hollingsworth et al., 2017, sample EmigZr7)
46.1 ± 0.2 Ma (Haynes, 2003, sample 00-188GS)
Elko Formation
Near Emigrant Spring (Fig. 3)
"Cherty limestone" of Mulch et al. (2015)
"Limestone and conglomerate" of Mulch et al. (2015)
δ18OSMOW (‰)
δ13CPDB (‰)

Figure 5. Isotopic analyses from Mulch et al. (2015) and sources therein plotted by stratigraphic section. Section and sample locations are shown in Figs. 3 and 4. Maximum depositional ages are indicated with inequality symbols ("≤"), unlike for nearly absolute depositional ages from interbedded tuffaceous horizons. Plotted stable isotope measurements and age data are listed in the GSA Data Repository. Values of $\delta^{18}O$ are reported relative to standard mean ocean water (SMOW) and values of $\delta^{13}C$ are reported relative to Peedee belemnite (PDB) for consistency with prior studies in this region. These plots complement those in Fig. 6, where isotopic measurements are plotted together by depositional age bounds.

REVIEW OF THE SEDIMENTARY AND VOLCANIC RECORD

Elko area of northeast Nevada

The Elko area is one of the only places in the Great Basin where well-preserved sedimentary and volcanic rocks spanning the Late Cretaceous(?) to Neogene are exposed over appreciable areas (e.g., Stewart, 1980). Because the term "Elko Basin," *sensu stricto*, refers to the part of northeast Nevada where the Elko Formation was deposited in Eocene time (see Camilleri et al., 2017), we use the term "ancestral Elko Basin" to refer to this general area over a wider time span.

As shown in Figure 6, little deposition is documented between the Cretaceous and early Eocene in the ancestral Elko Basin region (Smith and Ketner, 1976; Fouch et al., 1979; Rahl et al., 2002; Haynes, 2003; Crafford, 2007; Henry et al., 2011; Lund Snee and Miller, 2015), reflecting the history of gradual erosion that prevailed throughout much of the hinterland from the peak of Late Cretaceous deformation and magmatism until the middle Eocene (e.g., Van Buer et al., 2009; Konstantinou et al., 2012). The first strata deposited during this time span within the Elko area were Late Cretaceous(?) to early Eocene(?) redbeds and limestones (Figs. 3, 4c, 5, and 6), probably in isolated topographic lows, fault-bounded basins, or the bottoms of paleovalleys (Armstrong, 1968, 1972; Smith and Ketner, 1976; Gans and Miller, 1983; Van Buer et al., 2009; Konstantinou et al., 2012; Long, 2012; Lund Snee, 2013; Henry, 2018). These early deposits, as well as the overlying Elko Formation (Fig. 5), contain clast compositions and detrital zircon age distributions that reflect recycling from strata presently exposed beneath the Cenozoic unconformity (Druschke et al., 2011; Ruksznis, 2015; Lund Snee et al., 2016; Canada et al., 2020).

The more extensive middle to late Eocene Elko Formation (Figs. 5 and 6), which locally reaches thicknesses of ~850 m (Henry, 2008), consists of a broadly upward-fining succession of

conglomerate, sandstone, siltstone, shale, clay, marl, and limestone (Smith and Ketner, 1976; Solomon et al., 1979; Moore et al., 1983; Server and Solomon, 1983; Ketner and Alpha, 1992; Haynes, 2003; Lund Snee and Miller, 2015; Smith et al., 2017). The presence of Cenozoic tuffaceous material and other volcanic detritus is a key factor that distinguishes the Elko Formation from older units (Smith and Ketner, 1976; Lund Snee et al., 2016). Deposition of the Elko Formation began ca. 46.1 Ma (Fig. 5), based on a U-Pb zircon age of an ash-fall tuff deposited near its base (Haynes, 2003). The end of Elko Formation deposition is tightly constrained at ca. 38.4 Ma, based on a U-Pb detrital zircon maximum depositional age (MDA) of 37.9 ± 0.5 Ma from its upper stratigraphic levels within the eastern Carlin-Piñon Range, south of Robinson Mountain (Fig. 3; sample ELKO-2 of Lund Snee et al., 2016) and a minimum depositional age of 38.47 ± 0.15 Ma from $^{40}Ar/^{39}Ar$ plagioclase analysis on an overlying ash-flow tuff nearby (sample H10-45 of Henry et al., 2015) (Fig. 5). These dates revise an estimate of 40.4 Ma for the end of Elko Formation deposition by Smith et al. (2017) and they are compatible with estimates of ca. 39–38 Ma by Haynes (2003) and Mulch et al. (2015). The initiation of shallow basin development recorded by the onset of Elko Formation deposition ca. 46–44 Ma, shortly before arrival of volcanism (see below), indicates that volcanism occurring to the north in southern Idaho may have been responsible for a change in topography and regional stress state. The development of accommodation for deposition at this time, following tens of millions of years with little or no sedimentation, suggests initiation of a mechanism such as normal faulting, development of sags or uplifts, and/or establishment of broad paleodrainages (e.g., Howard, 2003; Smith et al., 2017; Henry, 2018; this study). Lithofacies characterization and $\delta^{13}C_{carbonate}$, $\delta^{18}O_{carbonate}$, and δD_{glass} measurements suggest that the Elko Basin experienced a profound transition in depositional setting between the lower and upper Elko Formation ca. 40 Ma, as volcanism became more proximal (Fig. 2), although published interpretations are contradictory. Mulch et al. (2015) suggested that elevations increased and lake waters freshened within the Elko Basin around this time, whereas Smith et al. (2017) proposed an upward transition from freshwater fluvial-lacustrine to saline and anoxic profundal settings, with substantial uplift only after the end of Elko Formation deposition.

The ca. 38.5–36.8 Ma Robinson Mountain volcanic field (Ressel and Henry, 2006; Henry et al., 2015; Lund Snee et al., 2016) is a thick succession (>1 km) of rocks associated with the ignimbrite flareup on the eastern flanks of the Carlin-Piñon Range (Fig. 3), and it conformably

overlies the Elko Formation (Smith and Ketner, 1976, 1978; Ressel and Henry, 2006; Ryskamp et al., 2008; Lund Snee and Miller, 2015). Following volcanism, sedimentation and faulting effectively ceased in this area (Fig. 6), with few exceptions, until Basin and Range faulting began in the middle Miocene (Henry et al., 2011; Lund Snee et al., 2016; this study). Any faulting that accompanied magmatism and crustal flow at depth might have been limited to the immediate areas above the metamorphic core complexes (MCCs), where the surface record is incomplete due to younger faulting and erosion (Miller et al., 1999; Colgan et al., 2010; Konstantinou et al., 2013a; Lee et al., 2017). Lund Snee et al. (2016) documented 10–15º tilting events following volcanism, between ca. 36.8–33.9 Ma and between ca. 31.1–24.4 Ma (better constrained by this study to between ca. 31.1–25.1 Ma as shown in Figs. 4b, 5, and 6), which they interpreted to represent local deformation associated with deeper crustal flow leading to surface adjustments by either faulting and/or doming adjacent to the developing Ruby Mountains–East Humboldt Range (REH) MCC. Best and Christiansen (1991) made a similar interpretation for the limited and localized faulting that occurred during the ~10 Myr following volcanism throughout the Great Basin.

An early phase of gradual extension within this generally quiescent interval may be represented by deposition of ca. 25 Ma and progressively younger fluvial-lacustrine material near the base of the Humboldt Formation (Figs. 3, 4a, and 6; Lund Snee et al., 2016; this study), as well as the possibly correlative late Oligocene and/or early Miocene sedimentary sequence of Clover Creek (McGrew and Snoke, 2015) near the East Humboldt Range (Fig. 1). Subsequently, rapid slip initiated on basin-bounding faults at 17–16 Ma (e.g., Colgan et al., 2010), represented in northeast Nevada by thick middle to late Miocene deposits of the Humboldt Formation. Near the REH (Figs. 3, 4b–d, and 5), the Humboldt Formation locally exceeds 4 km thickness (Satarugsa and Johnson, 2000), by far dwarfing the thicknesses of older Cenozoic units.

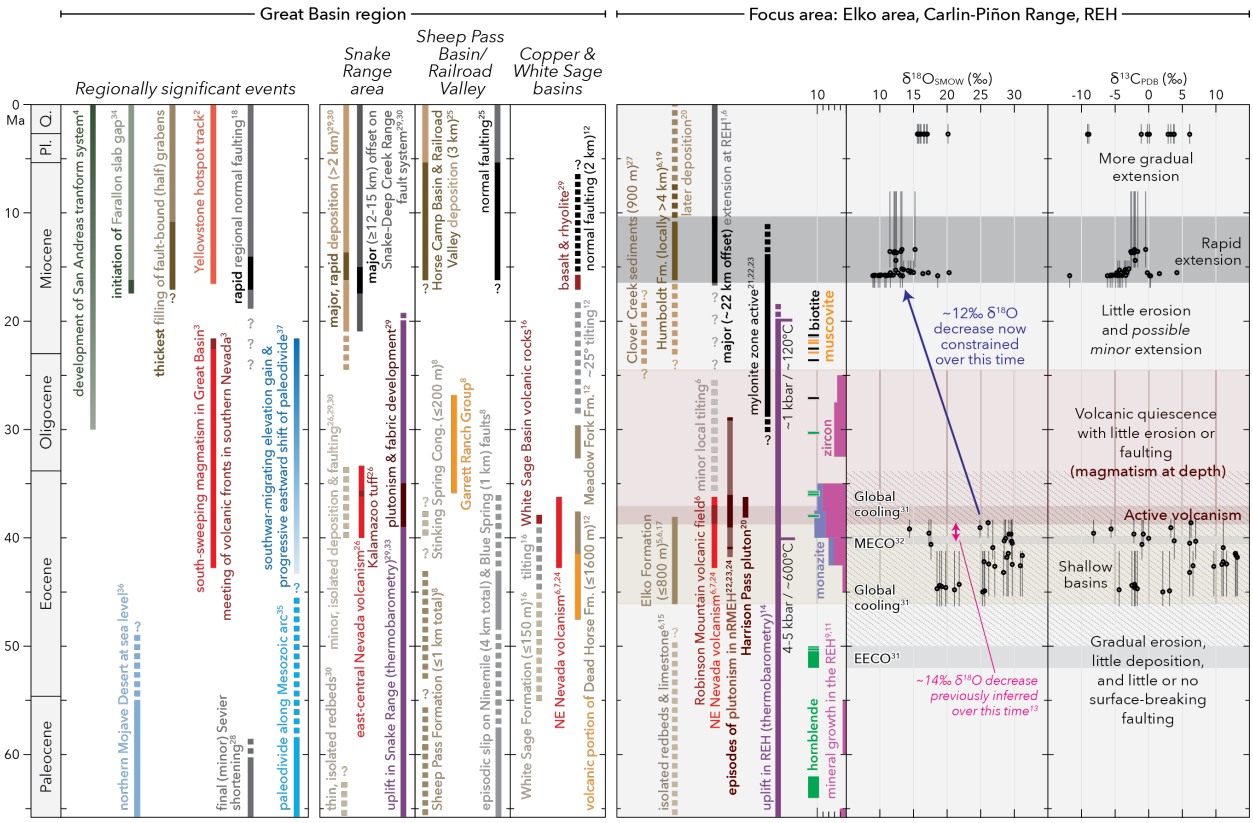

Figure 6. Regional Cenozoic tectonic events and measured isotopic values in the Elko area, northeast Nevada. Stable isotope data are from Mulch et al. (2015) and sources therein. Vertical bars indicate the full permissible age range for each analysis, conservatively including the 2σ uncertainties of the bounding age constraints. Values of $\delta^{18}O$ are reported relative to standard mean ocean water (SMOW) and values of $\delta^{13}C$ are reported relative to Peedee belemnite (PDB) for consistency with prior studies in this region. Cong.—Conglomerate; EECO—Early Eocene Climatic Optimum; Fm.—Formation; MECO—Middle Eocene Climatic Optimum; REH—Ruby Mountains–East Humboldt Range. References: 1—Colgan and Henry (2009); 2—Coble and Mahood (2012); 3—Armstrong and Ward (1991); 4—Atwater (1989); 5—Haynes (2003); 6—Lund Snee et al. (2016); 7—Brooks et al. (1995); 8—Druschke et al. (2009a, 2009b); 9—Howard et al. (2011); 10—Henry et al. (2011); 11—McGrew and Snee (1994); 12—Rahl et al. (2002) and McGrew et al. (2007); 13—Mulch et al. (2015); 14—McGrew et al. (2000); 15—Smith and Ketner (1976); 16—Potter et al. (1995) and Dubiel et al. (1996); 17—Henry (2008); 18—Stockli (2005); 19—Satarugsa and Johnson (2000); 20—Colgan et al. (2010); 21—Haines and Van Der Pluijm (2010); 22—Wright and Snoke (1993); 23—MacCready et al. (1997); 24—Ryskamp et al. (2008); 25—Horton and Schmitt (1998); 26—Gans et al. (1989); 27—McGrew and Snoke (2015); 28—DeCelles and Coogan (2006); 29—Miller et al. (1999); 30—Ruksznis (2015); 31—Zachos et al. (2001); 32—Sluijs et al. (2013); 33—Cooper et al. (2010); 34—Liu and Stegman (2012); 35—Van Buer et al. (2009); 36—Lechler and Niemi (2011); 37—this study.

Great Basin region

Here we expand the above discussion to include rocks of Late Cretaceous to Neogene age deposited elsewhere in the Great Basin, primarily in the Copper, White Sage, and Sheep Pass basins (Fig. 1). As can be seen in Figure 6, the histories of deposition and tectonism in these areas are broadly similar, characterized by limited and localized Late Cretaceous to Paleogene sedimentation and faulting (e.g., Gans and Miller, 1983; Best and Christiansen, 1991; Burchfiel et al., 1992; Van Buer et al., 2009; Henry et al., 2011; Konstantinou et al., 2012; Long, 2012; Henry and John, 2013) followed by volcanism, a subsequent hiatus in sedimentation, and then rapid sedimentation and tilting in the middle Miocene.

Regionally, the most significant deposition in the Late Cretaceous to Paleogene interval was in the greater Sheep Pass Basin of east-central Nevada (Fig. 1), where deposition of up to ~1200 m of Late Cretaceous–middle Eocene Sheep Pass Formation and late Eocene Stinking Spring Conglomerate (Fig. 6) was associated with potentially 3 km of normal slip on the northwest-dipping Ninemile fault system (Druschke et al., 2009a, 2009b). Sedimentation and tilting occurred elsewhere in east-central Nevada (Gans et al., 1989), including near the Snake Range MCC (Figs. 1 and 6), but deposition was localized (Best and Christiansen, 1991).

As in the case of the Elko area described above, the limited pre-Miocene deposition that did take place elsewhere in the Great Basin occurred several millions of years before ignimbrite flareup volcanism (Fig. 6), suggesting that early magmatic processes could have prompted changes in topography. In the Copper Basin of northeast Nevada (Fig. 1), localized late Eocene–Oligocene deposition may have occurred due to basin development associated with normal fault slip shortly before and during nearby volcanism (Axelrod, 1966; Rahl et al., 2002). Alternatively, these units (and the nearby Elko Formation) may have been deposited into paleochannels, some of which could have been partially dammed by faulting (Henry, 2008, 2018). In the White Sage Basin of western Utah, ~150 m of early Eocene deposits experienced modest tilting in the middle Eocene before being blanketed ca. 40–39 Ma by ignimbrite flareup volcanic rocks (Potter et al., 1995; Dubiel et al., 1996). These datasets appear to preclude significant activity and offset along Late Cretaceous to Oligocene faults, consistent with prior compilations for the Great Basin (Best and Christiansen, 1991; Colgan and Henry, 2009; Henry et al., 2011; Henry and John, 2013).

In most places, sedimentation effectively ceased following volcanism, lasting at least through most of the Oligocene. Similar to the REH MCC, gradual sedimentation near the Snake

Range MCC re-initiated as early as the late Oligocene or earliest Miocene (Miller et al., 1999; Ruksznis, 2015). Nevertheless, by far the most significant episode of sedimentation, tilting, and uplift in the Great Basin occurred during middle Miocene time, ca. 17–16 Ma, resulting in region-wide development of deep (often >2 km) half-graben basins that filled rapidly with sediments (Noble, 1972; Stockli et al., 2002; Colgan, 2013).

REVIEW OF STABLE ISOTOPE MEASUREMENTS

Numerous studies have targeted strata in the ancestral Elko Basin for stable isotope analysis in efforts to understand regional paleoelevation and paleoclimate histories (Fig. 3). Stable isotope measurements from Elko area carbonates have served as key constraints in regional studies arguing that large and rapid negative shifts in $\delta^{18}O$, which proceeded southward across the western USA approximately synchronous with migrating middle Cenozoic volcanism, indicate simultaneous south-migrating topographic uplift (Horton et al., 2004; Davis et al., 2006; Mix et al., 2011; Chamberlain et al., 2012), supporting a model initially proposed by Gans (1990). Specifically, these conclusions were based on a proposed ~7–10‰ decrease in $\delta^{18}O$ values at ca. 50–47 Ma in southwestern Montana and eastern Idaho (Kent-Corson et al., 2006), followed by a decrease of up to ~15‰ in the Elko Basin, proposed to have occurred between ca. 40.2–39.4 Ma (Mulch et al., 2015), and finally a ~4‰ decrease after ca. 23 Ma in southern Nevada (Chamberlain et al., 2012). This timing is generally corroborated by comparable negative shifts of $\delta^{18}O$ values ca. 44–40 Ma in foreland basin deposits east of the Sevier fold and thrust belt at the latitude of northeast Nevada (Fig. 1), which have been attributed to high-elevation catchment areas in the Sevier hinterland (e.g., Carroll et al., 2008; Davis et al., 2009). In the ancestral Elko Basin, the decrease in $\delta^{18}O$ values was interpreted to suggest 2.5 km of uplift occurring over <2 Myr (Chamberlain et al., 2012). Mulch et al. (2015) subsequently suggested that a component of the up to 15‰ decrease in $\delta^{18}O$ values in the Elko Basin should be attributed to climatic and diagenetic factors, including late Eocene global cooling.

More recently, however, the sedimentary age constraints, mean $\delta^{18}O$ values, and interpretations of depositional environment underpinning some of these studies have changed, both for the ancestral Elko Basin (Lund Snee et al., 2016; Smith et al., 2017) and the Sage Creek Basin of southwest Montana (Kent-Corson et al., 2010; Schwartz et al., 2019). In southwest Montana, Kent-Corson et al. (2010) revised the magnitude of the negative shift in $\delta^{18}O$ values

353 from 7‰ to only 4–5‰ (all $\delta^{18}O$ values are relative to standard mean ocean water, SMOW). The
354 4–5‰ shift was corroborated by Schwartz et al. (2019), who also established that it occurred
355 rapidly at ca. 47 Ma, across a conformable stratigraphic boundary. The ~1 Myr time interval for
356 this shift in $\delta^{18}O$ values may be too rapid to be explained by topographic changes associated with
357 Challis and Absaroka volcanism, which reached southwest Montana ~5 Myr earlier.
358 In the Elko area, Lund Snee et al. (2016) found that the rocks previously mapped as part
359 of the Oligocene Indian Well Formation (Fig. 3) are mostly middle Miocene and younger in age
360 and hence part of the Miocene Humboldt Formation. As a result, that study recommended
361 abandoning the Indian Well Formation name. Because much of the marked decrease in $\delta^{18}O$
362 values (an interpreted ~14–15‰ decrease from ~+29.1 to +14.4‰) occurred across this angular
363 unconformity, the age revisions imply that the timing of the shift could have occurred anytime
364 within a large window of time between 40–15.5 Ma. Our new geochronologic data and more
365 conservative approach to constraining temporal bounds (Fig. 6) do not significantly narrow the
366 time interval over which the $\delta^{18}O$ shift occurred, but they do constrain the ages more rigorously
367 and in greater detail than prior studies (e.g., Mix et al., 2011; Mulch et al., 2015; Lund Snee et
368 al., 2016; Smith et al., 2017). The record of $\delta^{18}O$ values with improved age constraints shown in
369 Fig. 6 indicates considerable scatter in $\delta^{18}O$ values both in the upper part of the Eocene Elko
370 Formation and in lower levels of the Humboldt Formation for which stable isotope values have
371 been measured. This scatter leads us to interpret a slightly different shift of ~–12‰, from ~+25
372 (but ranging between ~+14–+30‰) in upper Elko Formation strata with preferred ages spanning
373 ca. 40.9–38.6 Ma to ~+13‰ (ranging between ~+9–+20‰) in strata within the lower Humboldt
374 Formation with preferred ages spanning ca. 15.8–15.5 Ma. Although prior workers (e.g., Mulch
375 et al., 2015) argued that the decrease in $\delta^{18}O$ values occurred within the upper Elko Formation
376 because of a ~14–15‰ decrease that is observed within that succession, we point out that this
377 interpretation was made on the basis of three nonsequential data points and that $\delta^{18}O$ values
378 increase again by ~10‰ (from +14.4–+17.6‰ to +24.9–+26.1‰) immediately above and still
379 within the Elko Formation (Fig. 6). Such rapid oscillation of $\delta^{18}O$ values within a narrow part of
380 the succession are unlikely to reflect changes in topography. Hence, we conclude that the ~12‰
381 (or possibly less) decrease in $\delta^{18}O$ values observed in the Elko Basin occurred at an unknown
382 rate sometime between ca. 38.6–15.8 Ma. Moreover, our new age constraints and stratigraphic
383 thickness measurements show that >400 m of stratigraphic section are present below the lowest

384 measured Humboldt Formation $\delta^{18}O$ values, with a depositional age of 25.1 ± 0.2 Ma now
385 established for a tuffaceous bed near the base of that unit (Figs. 4 and 5). A consequence of the
386 improved age constraints is that we do not know when the decrease in Elko Basin $\delta^{18}O$ values
387 occurred relative to the onset of volcanism (Figs. 2 and 3) ca. 39–38 Ma (Ressel and Henry,
388 2006; Henry et al., 2015; Lund Snee et al., 2016). The sign and magnitude of the decrease in
389 $\delta^{18}O$ values is clearly consistent with an elevation increase, although it is also not definitive of
390 that because of the potential for climatic and diagenetic influences over this interval.
391 Stable isotopic studies focused instead on volcanic rocks erupted across the Great Basin
392 (including the Elko region) and westward to the Sierra Nevada flank have argued that a high
393 plateau persisted across the former Sevier hinterland between 41–23 Ma on the basis of relatively
394 low δD values in altered volcanic glass that span this age spectrum (Cassel et al., 2009, 2014,
395 2018). These results were interpreted to suggest that the inferred high plateau developed in
396 Cretaceous time (Henry et al., 2012). However, the δD values vary with sample age and location.
397 This led Cassel et al. (2018) to propose that elevations across the hinterland were ~2.25–3.0 km
398 during late Eocene time and then fell by ~0.5–1 km by early Oligocene time, followed by ~1.5
399 km uplift between the early and late Oligocene (to as high as 3.5 km in central Nevada), before
400 eventually falling to present-day mean elevations around 1.75 km. Although the presence of an
401 elevated plateau following the arrival of volcanism is consistent with the other geologic and
402 stable isotopic evidence discussed here, these proposed oscillatory elevation changes are difficult
403 to reconcile with geologic evidence as they imply multiple episodes of faulting and
404 sedimentation that are not corroborated by the geologic record (see above and summaries by Best
405 and Christiansen, 1991; Henry et al., 2011; Henry and John, 2013). Moreover, the age brackets of
406 $\delta^{18}O$ values from Elko Basin carbonates (Fig. 6; Horton et al., 2004; Mix et al., 2011;
407 Chamberlain et al., 2012; Mulch et al., 2015) are not consistent with models that require
408 elevations to have *decreased* between ca. 42–13 Ma (e.g., Coney and Harms, 1984; Sonder et al.,
409 1987; Bahadori et al., 2018; Cassel et al., 2018) because $\delta^{18}O$ and $\delta^{13}C$ values were generally
410 low from ca. 16 Ma onward and prior to ca. 42 Ma were substantially higher (Fig. 6).
411 In summary, recent work to improve age constraints and better define depositional
412 settings in both northeast Nevada and southwest Montana (Kent-Corson et al., 2010; Lund Snee
413 et al., 2016; Schwartz et al., 2019; this study) indicates that the stable isotope record does not
414 alone provide clear evidence for south-migrating topography across the region. On the basis of

more rigorous age constraints, the negative shift in $\delta^{18}O$ values within the ancestral Elko Basin cannot be decisively linked to the age of south-migrating volcanism, although it is consistent with uplift occurring at that time or later and is inconsistent with models requiring a decrease in elevation anytime between ca. 42–13 Ma (Fig. 6). Far stronger evidence for south-migrating topography is demonstrated by the other datasets discussed here: the record of sedimentation, faulting, erosion, and reorganization of drainage networks. Stable isotope studies based on δD values in altered volcanic glass present a more complex pattern with space and time. Published interpretations of those results cannot presently be reconciled with the existing record of sedimentation and faulting.

RE-EVALUATING THE EVOLUTION OF PRE-BASIN AND RANGE DRAINAGE SYSTEMS

Rocks preserved within a mapped network of Eocene–Oligocene paleovalleys (Fig. 2) provide additional insights for the region's topographic evolution that can be interpreted in concert with the sedimentary record. The paleovalleys are defined and mapped by their thicker sequences of volcanic fill and can be traced generally east–west from range to range across Nevada (Henry, 2008). The rocks filling the paleovalleys are precisely dated and consist of well correlated middle Cenozoic ignimbrites that flowed hundreds of kilometers east and west along these channels from their source calderas (e.g., Henry and John, 2013). The flow directions defined by these relations outline a north–south-trending paleodivide through central Nevada (Henry, 2008; Best et al., 2013), which has been widely displayed in subsequent publications portraying the paleotopography of the west. The paleodivide is viewed as a static feature at least through the early Cenozoic if not as far back as the Cretaceous (e.g., Henry et al., 2012).

Figure 2 shows the Cenozoic temporal evolution of volcanism together with the ages of oldest material dated within each paleodrainage (compiled from MacGinitie, 1941; Yeend, 1974; Goldstrand, 1992, 1994; Garside et al., 2005; Henry, 2008; Henry et al., 2012; Henry and John, 2013; Dumitru et al., 2015, 2016). The age of the oldest dated material in each paleovalley decreases systematically southward, broadly accompanied by the southward progression of volcanism. We consider it unusual that no basal paleovalley deposits have known ages significantly older than nearby magmatism. This is especially remarkable considering that the ignimbrites were capable of traveling hundreds of kilometers north and south of their eruptive

centers (Henry and John, 2013). For each stage of migrating volcanism, the earliest deposits are preserved near the source calderas, filling paleovalleys to the west, east, and sometimes north. Yet—critically—the record of fill preserved at the *bottoms* of paleovalleys (Fig. 2) shows few to no examples of eruptive products that would have had to travel significantly south (e.g., ≥100 km).

The likeliest explanation is that most or all of these drainages did not exist more than a few million years before magmatism began at a given latitude and paleovalleys were filled with volcanic material. We propose that the paleovalleys could have developed diachronously in response to dynamic topographic uplift that likely occurred during south-migrating ignimbrite flareup volcanism, when large amounts of magmatic material and thermal energy were added to the crust. In this context, fluvial paleovalleys with valley-margin relief approaching 1.2 km (e.g., Henry et al., 2012) were incised into the rising hinterland, similar to the paleovalleys that formed during the Paleocene–Eocene to the north of the study area (e.g., Schwartz and Schwartz, 2013; Schwartz et al., 2019). Migrating eruptions would have progressively filled any newly developed valleys with resistant volcanic rocks that eventually (because they blanketed the landscape) constructed an elevated, relatively flat plateau such as described by Best et al. (2009), with surface elevations substantially increased by magmatic and thermal input into the crust.

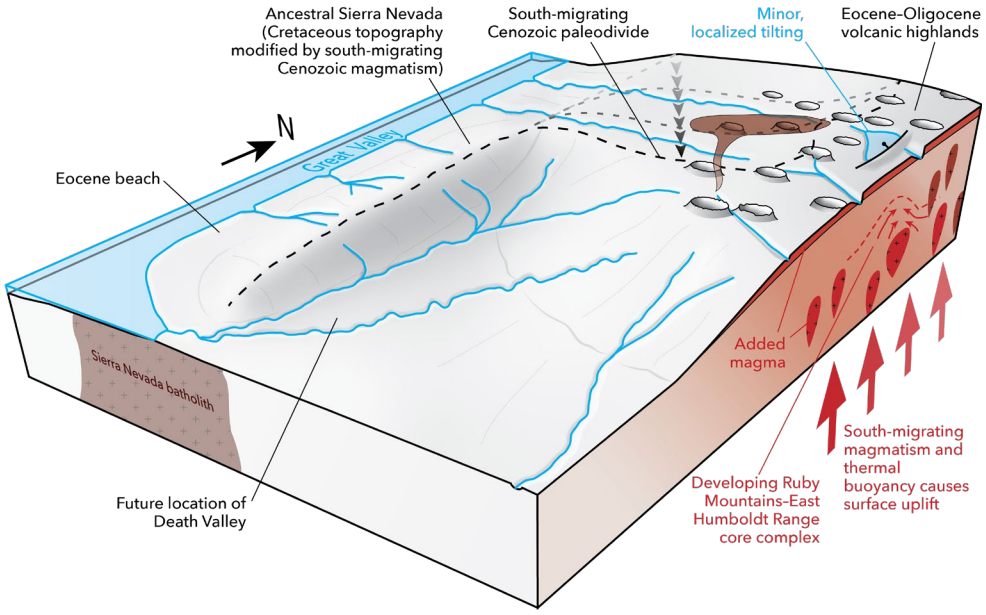

Figure 7. Schematic illustration of southward-migrating topographic uplift in the Great Basin related to the ignimbrite flareup. This figure depicts a late Eocene (ca. 36 Ma) snapshot of thermally and magmatically

supported volcanic highlands (to the north). At the latitude of the highlands, the drainage divide has shifted east from its Late Cretaceous to Paleocene position along the axis of the ancestral Sierra Nevada range (Van Buer et al., 2009) toward the center of the highlands. Latitudes farther south have not yet experienced surface uplift, and the divide remains along the ancestral Sierra Nevada range. Drainage networks have been reorganized near and north of the uplifted region, which remains elevated after cessation of volcanism due to input of substantial heat (as indicated by ongoing partial melting in the Ruby Mountains–East Humboldt Range metamorphic core complex; Fig. 6) and voluminous volcanic and plutonic material to the crust.

Figure 7 presents a schematic diagram of the proposed paleotopographic evolution ca. 36 Ma, immediately following the end of volcanism in the Elko area. As magmatism swept south across the Sevier hinterland in Eocene and Oligocene time, it prompted the growth of topography due to the voluminous addition of magma to the crust together with accompanying thermal uplift. We suggest that highlands developed near the main eruptive centers at any given time and that the ~north–south-trending paleodivide proposed by Henry (2008), Henry et al. (2012), and Best et al. (2013) was a southward-propagating dynamic feature, with the highest topography located above the region of the most active caldera centers. Prior to volcanism, drainages likely flowed east and west away from the axis of the Cretaceous arc (Figs. 2 and 6), as defined by the locus of intrusion of the youngest plutonic complexes (Van Buer et al., 2009; Van Buer and Miller, 2010; Sharman et al., 2015). This inference is based on the significantly higher calculated magnitudes of erosion (~5–7 km) in the arc compared to 1–3 km across the back-arc region west of the Sevier fold and thrust belt (Van Buer et al., 2009). The detrital zircon signatures of Late Cretaceous–Eocene sediments deposited in the California forearc basin, west of the arc axis, also indicate derivation from the Sierra Nevada magmatic arc (Figs. 1 and 2) and do not indicate detectable sediment derivation from farther east (Sharman et al., 2015). Some drainages may also have flowed southward toward the Mojave region (Fig. 1), much of which was a marine environment during Paleocene time (e.g., Lofgren et al., 2008; Lechler and Niemi, 2011). Evolving southward-moving uplift would have tended to reorganize pre-existing topography and drainages that were holdovers from the Late Cretaceous, resulting in paleodrainages that emanated to the west, east, and south from the new paleodivide in Nevada (e.g., Best et al., 2013; Henry and John, 2013; Lechler and Niemi, 2011; Miller et al., this volume). Notably, exposures of the Eocene Titus Canyon Formation in the Funeral Range, southeast California (Fig. 1), herald the onset of volcanism in north central Nevada and include clast compositions and detrital zircon

499 age components that suggest that sediment traveled through this region in south-flowing river
500 systems from higher elevations located at least 300 km to the north-northeast (Miller et al., 2019;
501 Miller et al., this volume). At the same time, paleodrainages were unlikely to flow northward
502 from active calderas due to the presence of predecessor high topography (Fig. 7).
503 Removal of the Farallon slab during middle Cenozoic time is thought to have caused the
504 asthenospheric upwelling and subsequent ignimbrite flareup magmatism that would have also
505 thinned the lithosphere below the Great Basin (Humphreys, 1995). Thermally driven uplift is an
506 established consequence of both lithospheric thinning and addition of magmatic material (e.g.,
507 Lachenbruch and Morgan, 1990). The precise magnitude of elevation increase due to ignimbrite
508 flareup volcanism is uncertain, but analogy with other regions suggests that it was 1 km or more
509 (see Crough, 1978; Pierce and Morgan, 1992; Larimer et al., 2019; Schwartz et al., 2019). Along
510 and adjacent to the Yellowstone hotspot track (approximately the Snake River Plain on Fig. 1),
511 localized volcanism between middle Miocene time and the present was accompanied by an east-
512 migrating zone of pronounced uplift, faulting, reorganization of drainage systems, and shifts of
513 the continental divide (Anders and Sleep, 1992; Pierce et al., 1992; Beranek et al., 2006; Coble
514 and Mahood, 2016; Camilleri et al., 2017; Larimer et al., 2019). Detrital zircon records indicate
515 that northeastward migration of Yellowstone hotspot magmatism profoundly disrupted drainage
516 networks, causing streams to emanate away from the associated topographic bulge as it
517 progressed, producing a northeast-oriented paleodivide that was centered either on or at the
518 southern margin of the hotspot track, which later evolved into a crescent-shaped divide around
519 the northwest, east, and southeast sides of Yellowstone (Beranek et al., 2006; Camilleri et al.,
520 2017). The uplift near Yellowstone has led to 1 km deep river incision since 3.6 Ma, an incision
521 rate of nearly 300 m/Myr (Pierce and Morgan, 2009). If the middle Cenozoic Great Basin
522 paleovalleys shown in Fig. 2 developed as a result of magmatism as we propose, then the up to
523 1.2 km of mapped paleovalley relief (Henry, 2008; Henry et al., 2012) provides a minimum
524 estimate for the amount of syn-volcanic uplift, comparable to recent incision near Yellowstone.
525 The lack of evidence for paleorivers that incised into this elevated volcanic tableland following
526 the decline of volcanism (Figs. 6 and 7) might have been a consequence of post-volcanic areas
527 being slightly lower than areas to the south that were still experiencing active volcanism, and/or
528 due to the erosional resistivity of the volcanic rocks. The uplift rates along the Yellowstone
529 hotspot track not only demonstrate the significance of thermally driven topographic changes but

also underscore that hundreds of meters of paleovalley erosion/incision may occur relatively rapidly, such as on the order of 1 to 10 Myr, rather than over long periods of geologic time, such as from the Late Cretaceous to middle Eocene (see, e.g., Colgan and Henry, 2017). We propose that the same processes that are active today near Yellowstone were active in the Great Basin, but at a grander scale, during the much more voluminous middle Cenozoic ignimbrite flareup.

PALEOGEOGRAPHIC EVOLUTION OF NORTHEAST NEVADA AND THE GREAT BASIN

Based on the evidence presented above from the sedimentary, structural, and magmatic records of the Elko area, integrated with data from surrounding areas, we present a summary view of the evolution of the Late Cretaceous to Cenozoic paleogeography of the northern Great Basin, as illustrated in Fig. 8. The timeline applies to northeast Nevada (right-hand panels of Fig. 6), but we suggest that it is also applicable to much of the Great Basin, especially where pertaining to regional tectonic events (left-hand panels of Fig. 6). This paleogeographic and tectonic history is based upon the well-preserved and less controversial surface geologic record, but it is also intended to reconcile some of the contradictory models for the tectonic evolution of the region.

Late Cretaceous to middle Eocene (until ca. 46 Ma): Gradual erosion

Surface-breaking thrust faults were active along the Sevier belt (Fig. 1) in the Late Cretaceous (Fig. 8a), and they created topography as the thrust belt finalized its development and shed its erosional debris into the foreland basin (e.g., Malone et al., this volume). In addition to voluminous foreland basin deposits, erosion of the Sevier belt is reflected by the basal Cenozoic unconformity map that shows erosion carved much deeper into the miogeoclinal section within the thrust belt (e.g., Armstrong, 1968, 1972; Van Buer et al., 2009; Konstantinou et al., 2012). The Sevier thrust faults ceased most of their motion by Paleocene time (Fig. 6) as deformation moved east to the Rocky Mountains during the middle Late Cretaceous to Eocene Laramide orogeny (e.g., DeCelles and Coogan, 2006; Copeland et al., 2017), but motion along the Paris thrust of the Sevier belt in southeast Idaho and northeast Utah may have continued into the Oligocene (Malone et al., this volume). The switch to Laramide-style deformation is thought to be linked to the onset of shallow slab subduction of part of the Farallon plate (Fig. 8a), as

561 documented by both the cessation of magmatism in the Sierra Nevada arc and the eastward shift
562 of deformation (e.g., Dickinson and Snyder, 1978).
563 Throughout the Late Cretaceous and early Cenozoic (Fig. 6), northeast Nevada and much
564 of the Great Basin region to the west of the Sevier thrust belt (its hinterland) appears to have
565 experienced only modest erosion (less than 3 km in most areas) with evidence for faulting and
566 tectonism in the surficial record only located around a handful of previously identified structures
567 (e.g., Van Buer et al., 2009; Konstantinou et al., 2012; Long, 2012). These inferences are farther
568 supported by reconstructions of the middle Cenozoic unconformity and paleogeologic maps of
569 units beneath that unconformity. The observation of generally low conodont alteration index
570 values across much of the Great Basin (Harris et al., 1980; Gans and Miller, 1983; Gans et al.,
571 1990; Crafford and Harris, 2005) likewise indicates burial only to stratigraphic depths and is
572 consistent with erosion mostly limited to the upper part of the Paleozoic-Mesozoic shelf
573 stratigraphic section. During the Late Cretaceous and early Cenozoic, multiple lines of evidence
574 discussed above suggest that the regional topographic divide was located near the axis of the
575 Cretaceous magmatic arc (Figs. 2, 6, and 8a; Van Buer et al., 2009; Sharman et al., 2015). To the
576 east of the Sevier fold and thrust belt, parts of the foreland basin system in Utah were near sea
577 level (Fig. 8a) in the Late Cretaceous (DeCelles and Coogan, 2006). The southern margin of the
578 Great Basin also lay near sea level in Paleocene and possibly early Eocene time (Figs. 1 and 6),
579 as indicated by the Paleogene marine fossils near the southeastern part of the Sierra Nevada, on
580 the northern margin of the Mojave Desert (Lofgren et al., 2008; Lechler and Niemi, 2011).
581 Consequently, elevations most likely decreased both to the east (Fig. 8a) and south from the
582 Cretaceous Sierra Nevada arc and the Sevier hinterland.
583
584 **Middle Eocene (ca. 46–38 Ma): Shallow basins and early volcanism in northeast Nevada**
585 The Elko and Copper basins developed during middle Eocene time as shallow basins in
586 northeast Nevada (Figs. 1 and 2), initiating by ca. 46 Ma and perhaps locally as early as ca. 49
587 Ma (Haynes, 2003; Lund Snee et al., 2016; Smith et al., 2017). At about this time, the Farallon
588 shallow slab is inferred to have started to steepen (Fig. 8b), triggering upwelling of hot
589 asthenosphere that contributed to an influx of magma and heat to the crust (e.g., Armstrong and
590 Ward, 1991; Humphreys, 1995; Konstantinou et al., 2012; Konstantinou and Miller, 2015). The
591 Elko and Copper basins (Fig. 1) provide the first indications of an eastward shift of the

topographic divide (Fig. 8b) in middle Eocene time. Deposits preserved in paleovalleys indicate both eastward and westward flow of ignimbrites away from an area west and north of the Elko Basin (Fig. 2) in northern Nevada (Henry, 2008). As suggested above, the mapped paleodrainages developed approximately during magmatism (Fig. 6), changing an earlier landscape through topographic growth and reorganizing and replacing pre-existing drainage networks (Fig. 7).

Basin development may have been a result of normal faulting (Vandervoort and Schmitt, 1990; Rahl et al., 2002; Haynes, 2003; Howard, 2003) and/or isostatic adjustments associated with steepening of the Farallon slab and associated asthenospheric upwelling (Smith et al., 2017) and/or the onset of magma chamber formation and volcanism. Faulting before and during ignimbrite flareup volcanism "was minor and/or exceedingly local" throughout the Great Basin (e.g., Henry and John, 2013, p. 954), but such faulting shortly before—and in rare cases during—volcanism is observed in several areas, including northeast Nevada (e.g., Henry et al., 2011) and central Nevada (e.g., Gans et al., 1989; Best and Christiansen, 1991; Miller et al., 1999; Druschke et al., 2009a; Ruksznis, 2015). Localized faulting may have occurred due to rapid but differential emplacement of voluminous magma bodies and heat transfer to the upper crust, and/or to localized thermal weakening of crust experiencing far-field extensional strain, as has been suggested for the vicinity of all three Great Basin MCCs (Miller et al., 1999; Konstantinou et al., 2012, 2013a; Konstantinou and Miller, 2015; Lund Snee et al., 2016; Lee et al., 2017). Arrival of volcanism was accompanied by a marked increase of heat input to the crust as indicated by increased high-T mineral (zircon and monazite) growth ca. 42 Ma at deeper levels of the crust now exposed in the REH MCC (Fig. 6; Howard et al., 2011).

Late Eocene (ca. 38–36 Ma): Active magmatism with volcanism

Sedimentation effectively ceased with the inception of volcanism (see above and Fig. 6), which blanketed the focus area with volcanic flows and ignimbrites beginning ca. 38 Ma (Haynes, 2003; Ressel and Henry, 2006; Lund Snee et al., 2016). These volcanic rocks formed a flat regional tableland (Best et al., 2009) that persisted in northeast Nevada with little erosion until the onset of Neogene Basin and Range faulting. Similar relationships are likely across the entire northern Great Basin (Fig. 6), as documented by the widespread preservation of volcanic rocks above the regional lower Cenozoic unconformity (e.g., Gans and Miller, 1983; Van Buer et

al., 2009; Konstantinou et al., 2012). Following the last eruption within the study area ca. 36.8 Ma (Lund Snee et al., 2016), magmatism continued southward (e.g., Ryskamp et al., 2008), likely in tandem with elevation gain, as proposed in this paper (Fig. 7).

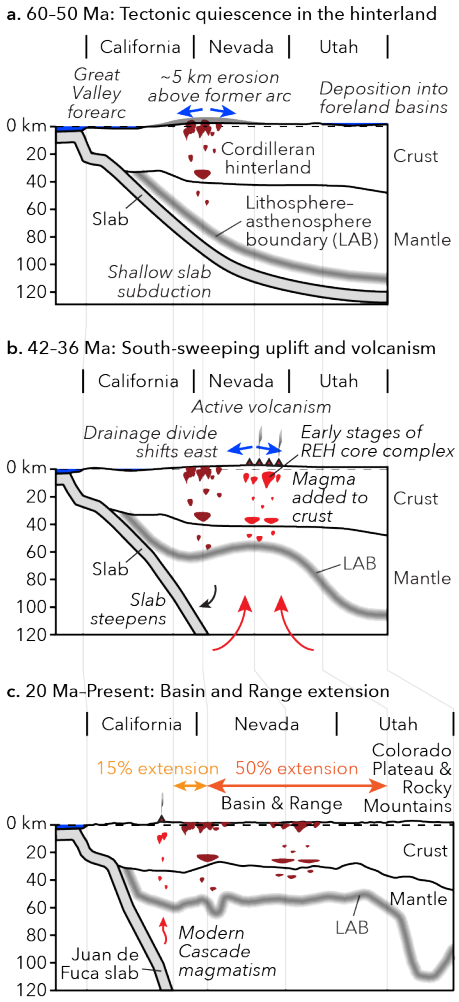

Figure 8. Cross sections along 40.5ºN latitude (line of section shown in Fig. 1) from Late Cretaceous time to the present. Present-day crustal thickness is from Shen and Ritzwoller (2016), the lithosphere–asthenosphere boundary is after the combined Sp–Ps interpretation of Levander and Miller (2012), and the Juan de Fuca slab position is after McCrory et al. (2012) and Tian and Zhao (2012). Extension magnitudes are based loosely on those estimated by Colgan et al. (2004) and Colgan and Henry (2009).

Late Eocene to latest Oligocene (ca. 36–25 Ma): Volcanic quiescence with little erosion or faulting at the Earth's surface (but continuing magmatism and crustal melting at depth)

Partial melting and magmatism continued in the deeper crust within the developing REH MCC and the Albion–Raft River–Grouse Creek (ARG) MCC to the north (Figs. 1, 2, and 6), long after the cessation of surface volcanism, and concomitant with relative rise of metamorphic rocks (McGrew and Snee, 1994; McGrew et al., 2000; Howard et al., 2011; Konstantinou et al., 2013a). The persistence of elevated temperatures, combined with ongoing and prior magmatic addition to the crust from the mantle, likely ensured that topography remained thermally elevated to some degree (Fig. 7), at least through much of the Oligocene. The near absence of sedimentary deposits between ca. 38–25 Ma in the study area (Fig. 6) and following volcanism throughout the northern Great Basin in general (Henry et al., 2011) confirm that whatever surface-breaking faulting that occurred during the 10 Myr or more time span following volcanism was very limited in extent and magnitude.

Latest Oligocene to middle Miocene (ca. 25–16.5 Ma): Little erosion and limited faulting

The sedimentary record in northeast Nevada indicates that tectonic quiescence and gradual erosion occurred between latest Oligocene and middle Miocene time (Fig. 6). Locally, however, lacustrine sedimentation (indicating the formation of basin accommodation) may have initiated (Figs. 4b, 5, and 6), based on ages of the earliest fluvial-lacustrine sediments deposited above Eocene and Oligocene volcanic rocks in Huntington Valley (Figs. 4b and 5) and near the East Humboldt Range (Fig. 1) (Frerichs and Pekarek, 1994; McGrew and Snoke, 2015; Lund Snee et al., 2016). Minor deposition in the latest Oligocene or early Miocene has also been recorded near the Snake Range MCC (Gans et al., 1989; Miller et al., 1999; Ruksznis, 2015) and elsewhere (Fig. 6).

Middle Miocene (17–16 Ma) to present: Rapid and then more gradual extension

As discussed above, rapid slip on Basin and Range normal faults with formation of ensuing topography similar to that of today occurred across most of the central part of the northern BRP (Figs. 1, 2, 6, and 8c) ca. 17–16 Ma (e.g., Noble, 1972; Lund et al., 1993; Miller et al., 1999; Stockli, 2005; Colgan et al., 2010). Across this region, fault slip rates decreased beginning ca. 12–10 Ma (Fig. 6), based on thermochronologic data and sedimentation rates (e.g., Colgan et al., 2008; Colgan and Henry, 2009). Extension that began in these central areas subsequently propagated west, east, and north (Surpless et al., 2002; Stockli, 2005; Colgan et al.,

2006; Lerch et al., 2008). Extension continues at a slow rate today as active slip takes place primarily on faults now close to the boundaries of the province (Thatcher et al., 1999; Kreemer et al., 2010). The timing of rapid extension coincides closely with a number of notable tectonic events (Figs. 6 and 8c), including final removal of the Farallon slab ca. 20 Ma (Humphreys, 1995), development of a gap in the Farallon slab ca. 17 Ma and subsequent impingement of the Yellowstone hotspot (Liu and Stegman, 2012), and the progressive development of the San Andreas transform boundary with northward migration of the Mendocino triple junction over Neogene time (Atwater and Stock, 1998).

IMPLICATIONS FOR PALEOTOPOGRAPHY AND CRUSTAL THICKNESS

The paleogeographic and crustal history outlined in the above synthesis (Figs. 6, 7, and 8) has direct implications for the topographic and crustal evolution of the hinterland region between the Cretaceous arc and Sevier thrust belt (Figs. 1 and 2). Multiple lines of evidence suggest that appreciable elevation gain (probably 1 km or more, as suggested above) may have taken place much later than Mesozoic time (Fig. 8a), roughly synchronous with and persisting to some degree after Cenozoic volcanism swept across the region (Figs. 2 and 8b), before subsiding to its present ~1.5–2.0 km average elevations and sawtooth topography during and/or after Basin and Range extension (Fig. 8c). The growing database discussed here indicates an important time lag between crustal thickening and extension that is inconsistent with suggestions that a high plateau was supported by gravitationally unstable crust overthickened during the Mesozoic (e.g., Sonder et al., 1987; Chase et al., 1998; Druschke et al., 2009b; Wells et al., 2012; Wells and Hoisch, 2012; Affinati et al., this volume). In addition, an important consideration is that the heat budget represented by ultimately mantle-derived Cenozoic magmatism by far exceeded that related to thermal equilibration of crust thickened by thrust faulting (Gottlieb, 2018; Gottlieb et al., this volume).

The thermal effects from voluminous and widespread ignimbrite flareup magmatism are rarely considered in topographic and tectonic models of the Great Basin. Studies that estimate pre-extensional crustal thicknesses by restoring Cenozoic extension (e.g., Bahadori et al., 2018; Long, 2018) do not account for the substantial thicknesses of middle Cenozoic volcanic material added to the surface in many areas nor the potentially much greater volumes of associated plutonic material; thus, their inferred post-thickening and pre-extensional crustal thicknesses are

likely overestimates. A (map view) restoration of topography across the northern Great Basin by Bahadori et al. (2018) proposed a narrow, tall (crest ≥4 km and peaks >6 km) mountain range atop a ~55–60 km thick welt of crust in the Eocene. That study restored pre-extensional crustal thicknesses based on the kinematic model by McQuarrie and Wernicke (2005), combined with an isostatic compensation model. The geometry of the resulting crustal welt is broadly similar to that shown by Long (2018), which was based largely on the Sevier thrust belt reconstruction of DeCelles and Coogan (2006). The modeled mountain chain by Bahadori et al. (2018) lies ~200 km east of the middle Cenozoic paleodivide that was inferred by Henry et al. (2012) and Best et al. (2013) using the paleoflow directions of channelized ignimbrites. The suggestion of a rugged, ≥4 km-tall mountain chain along the Utah-Nevada border, supported by relatively thick crust, is at odds with evidence that pre-volcanic erosion magnitudes were modest and smoothly distributed throughout the area of the inferred crustal welt (Gans and Miller, 1983; Miller and Gans, 1989; Konstantinou et al., 2012; Long, 2012). It would also be unusual for such steep topography to develop just to the west of the active fold and thrust belt. This disagreement between these estimates of crustal thickness and topography and the geologic data described in this paper suggests the need for (1) Retrodeformation studies that consider the limited crustal thicknesses that lay beneath the passive margin sequence west of its depositional hingeline; (2) Tighter constraints on the magnitude of westward crustal underthrusting (see Craddock et al., this volume; Gottlieb et al., this volume); (3) Incorporation of updated models of Cenozoic extension and possible magmatic additions to the crust during the ignimbrite flareup; and (4) Consideration of the thermal state of the crust and the likelihood of regional-scale lower crustal flow that might flatten the Moho before and during extension (Gans, 1987).

The assortment of geologic data presented here is incompatible with suggestions that crustal thicknesses became so great during Mesozoic shortening that they led to gravitationally driven extensional collapse (e.g., Wells et al., 2012). There is also little in the record of sedimentation, stable isotope values, and deformation such as surface faulting to suggest significant changes in elevation between the Late Cretaceous and shortly before the arrival of middle Cenozoic volcanism. What little deposition occurred was mostly within the Sheep Pass Basin, where up to ~1 km of Sheep Pass Formation sediments was deposited throughout Late Cretaceous to middle Eocene time (Figs. 1, 2, and 6; Druschke et al., 2009a, 2009b). We point out that the gradual, localized occurrence of normal faulting thought to have provided

accommodation for these deposits need not signify wholesale gravitational collapse of overthickened crust across the immense region envisaged as encompassing the *Nevadaplano*. Moreover, topographic relief (which would result from widespread surface-breaking faulting) likely was low across most of the Sevier hinterland before middle Cenozoic time (Fig. 8a), based on the depositional patterns of far-traveled Cenozoic ash-flow tuffs (e.g., Best et al., 2009) and the modest magnitudes of pre-Eocene erosion and tilting documented in the Elko region (Brooks et al., 1995; Henry et al., 2011; Lund Snee et al., 2016; Canada et al., 2019; this study) and across the hinterland in general (Gans and Miller, 1983; Gans et al., 1990; Crafford and Harris, 2005; Van Buer et al., 2009; Long, 2012; Konstantinou et al., 2013b). Suggestions that the hinterland was early on characterized by rugged, mountainous topography (Druschke et al., 2011; Bahadori et al., 2018; Bahadori and Holt, 2019) are clearly at odds with the above set of observations.

Few constraints are available for absolute elevations of the Sevier hinterland prior to extension, during the Late Cretaceous and early Cenozoic. Measurements from Eocene fossil leaves in Copper Basin (Figs. 1 and 2), representing the time at the onset of volcanism, provide widely distributed elevation estimates ranging from 0.6–1.2 km (Christiansen and Yeats, 1992) and 1.6 ± 1.6 km (Chase et al., 1998), to 2.0 ± 0.2 km (Wolfe et al., 1998) and 2.8 ± 1.8 km (Chase et al., 1998). This broad range complicates efforts to employ such estimates quantitatively. A definitive minimum hinterland elevation bound of 1.2 km was provided by Henry et al. (2012), based on measured middle Cenozoic paleovalley depths, which we suggest developed only after uplift related to ignimbrite flareup volcanism. Probably the most reliable estimates of absolute elevation are provided by two clumped isotope studies. Snell et al. (2014) estimated that absolute elevations in the Sheep Pass Basin (Fig. 1) of east-central Nevada ranged between 2.0–3.1 km in latest Cretaceous to early Paleocene time. Also using clumped isotope thermometry, Lechler et al. (2013) estimated only ≤2 km paleoelevation for the Sheep Pass Basin, integrated over the younger but overlapping latest Cretaceous–early Eocene interval. Although different, these two elevation estimates overlap at ~2 km, suggesting that this may be a reasonable elevation value for east-central Nevada in latest Cretaceous–early Eocene time. Additional lines of evidence support suggestions of only modest elevations across the Sevier hinterland prior to volcanism. As noted, marine fossils, stable isotope data, and detrital populations show that the southern Sierra Nevada and areas slightly to the east (~35.5ºN

latitude), which have a similar geologic history to the Great Basin, were *at or near sea level* in the Paleocene (Figs. 1 and 6) and may have remained very low (<1 km) into Eocene time (Lofgren et al., 2008; Lechler and Niemi, 2011). If a significantly elevated plateau was present across the Great Basin in Late Cretaceous and Paleogene time, then it must have been limited to areas north of ~37–38ºN and bounded on the south by slopes leading nearly to sea level.

It is challenging to reconcile the above narrative of Great Basin surface evolution with implications for 10–20 km of relative uplift implied by quantitative geobarometry on Cretaceous metamorphic assemblages in MCCs (Hodges et al., 1992; Lewis et al., 1999; McGrew et al., 2000; Cooper et al., 2010; Hallett and Spear, 2013). These analyses represent the primary evidence supporting suggestions of large crustal thicknesses that drove gravitational collapse of the hinterland prior to Miocene time. A more complete discussion of these questions is provided by Hoiland et al. (this volume), but two hypotheses are relevant: 1.) In recent years, it was recognized that the assumptions underpinning these geobarometric methods may in some cases be invalid, particularly the expectations that mineral assemblages were in equilibrium during formation (Spear et al., 2014) and that the pressure measurements can be interpreted as representing steady-state overburden pressures (proportional to burial depth) rather than transient and/or non-isostatic (tectonic) stresses (Schmalholz et al., 2014; Gerya, 2015). This leaves open a number of other possibilities to explain high pressure estimates in Great Basin MCCs, including tectonic "overpressure" (Henry et al., 2018; Thorman et al., 2020; Zuza et al., 2020; Hoiland et al., this volume). 2.) If some or all of the proposed uplift in developing MCCs was Cenozoic in age, then uplift could have occurred with little surface-breaking extension provided that lower crustal rocks were locally decoupled from surface deformation due to strongly elevated heat flow during mid-crustal melting (MacCready et al., 1997; Miller et al., 1999; Konstantinou et al., 2012; Lund Snee et al., 2016; Lee et al., 2017). This mechanism would explain the difference in timing of subsurface uplift versus surface-breaking extension, as elegantly demonstrated for the ARG (Fig. 1) MCC (Konstantinou et al., 2013a).

CONCLUSIONS

We have presented an updated view of the enigmatic transition from Mesozoic shortening to Cenozoic extension in the Great Basin (Figs. 1 and 2), focusing primarily on the supracrustal records of sedimentation, erosion, faulting, volcanism, and stable isotope values, and how those

relate to topography development. This integrated record shows that gradual erosion, limited deposition, and general tectonic quiescence prevailed between Late Cretaceous and middle Cenozoic time (Fig. 6). Although surface-breaking faults are documented across this time interval, they were local in scale and significance, involving relatively low magnitudes of slip (e.g., Best and Christiansen, 1991; Henry et al., 2011). The arrival of south-migrating ignimbrite flareup volcanism in the middle Cenozoic profoundly affected topography, disrupting hinterland drainage networks. This is most clearly shown by the systematic southward-younging ages of the oldest material recorded at the base of west- and east-flowing Eocene–Oligocene paleovalleys (Fig. 2), suggesting that new drainages formed progressively southward, roughly synchronous with volcanism. In some areas, volcanism was also preceded by development of shallow basins, relatively minor offset along normal faults, and limited sedimentation. We suggest that volcanism caused pronounced uplift, perhaps of the order of 1.2 km based on the measured height of paleovalleys active during this time (Henry et al., 2012). Given the massive influx (see, e.g., Best et al., 2009) of heat associated with the addition of volcanic and plutonic material to the lithosphere, uplift is an expected result (e.g., Lachenbruch and Morgan, 1990), as exemplified today by the >1 km uplift around Yellowstone (e.g., Pierce et al., 1992). However, while the records of sedimentation, erosion, faulting, drainage development, and magmatism all support an elevation increase associated with the ignimbrite flareup, this is no longer clearly supported by the available stable isotope information from carbonates in basins across the western USA. A consequence of the improved age control and characterization of those sections near Elko (Lund Snee et al., 2016; Smith et al., 2017; this study) and in southwest Montana (Schwartz et al., 2019) is that prominent decreases in $\delta^{18}O$ values during the early and middle Cenozoic (e.g., Horton et al., 2004; Davis et al., 2006; Kent-Corson et al., 2006; Mix et al., 2011; Chamberlain et al., 2012) can no longer be tied directly to the onset of volcanism in these areas.

We propose that dynamic uplift accompanying ignimbrite flareup magmatism shifted the continental divide eastward into central Nevada from its prior position along the crest of the Cretaceous magmatic arc (Van Buer et al., 2009) and that this shift occurred in a southward-propagating fashion (Figs. 7 and 8). The middle Cenozoic highlands that supported this developing paleodivide were not static but instead responded dynamically as eruptions occurred and calderas formed. Volcanism left behind a plateau, with little documented erosion, tectonism, or sedimentation occurring until ca. 17 Ma (Figs. 6–8), although minor deposition initiated as

early as latest Oligocene time in certain areas (Fig. 6), dominantly near developing metamorphic core complexes (Gans et al., 1989; Frerichs and Pekarek, 1994; Miller et al., 1999; Lund Snee et al., 2016; McGrew and Snoke, 2015; Ruksznis, 2015; this study). Elevations likely remained high following volcanism (perhaps with some component of gradual subsidence) due to the largely irreversible addition of magma to the crust and evidence that rocks currently exposed in MCCs experienced partial melting tens of millions of years later than the onset of Cenozoic magmatism (Howard et al., 2011; Strickland et al., 2011; Konstantinou et al., 2012, 2013a; Konstantinou and Miller, 2015). Rapid regional extension by Basin and Range faulting initiated ca. 17 Ma (Stockli, 2005; Colgan and Henry, 2009; Colgan, 2013), probably in response to changing boundary conditions, and driven by crust that remained elevated and thermally weakened.

The tectonic and topographic history and its temporal framework discussed here challenge suggestions that Mesozoic shortening produced a greatly thickened and elevated crust that drove gravitational collapse across the Sevier hinterland either during shortening or soon after (see also Konstantinou, this volume). Evidence for rapidly evolving topography, drainage divides, and highlands related to and during Cenozoic magmatism also challenges the traditional notion of a long-lived, strongly elevated *Nevadaplano* (Cassel et al., 2012; Wells et al., 2012; Best et al., 2013) with a fixed (Late Cretaceous to) Cenozoic drainage divide (Henry et al., 2012). These suggestions pose implications for our understanding of orogenic and magmatic systems worldwide, underscoring the short time scales over which major changes in elevation and catchment can occur, particularly when the influence of magmatism on topography is considered.

ACKNOWLEDGEMENTS

We thank Trevor A. Dumitru for guidance with detrital zircon geochronology, Mark E. Raftrey for analyzing four detrital zircon samples, and Stephen Pearcey and Virginia Isava for assisting with sampling. The manuscript benefitted from discussions with Simon L. Klemperer, George A. Thompson, Joseph P. Colgan, Karen I. Lund, Norm H. Sleep, and Theresa M. Schwartz. We are grateful to John P. Craddock for thoughtful editorial work and to Kathryn E. Snell, Theresa M. Schwartz, and David H. Malone for detailed comments that considerably

improved the manuscript. This research was funded by NSF grant EAR-1322084 to Miller and a Stanford University G.J. Lieberman Fellowship to Lund Snee.

REFERENCES

Affinati, S.C., Hoisch, T.D., Wells, M.L., and Wright, S., 2021, Timing of Jurassic burial and exhumation in the hinterland of the Sevier orogen in Barrovian metamorphic rocks dated by monazite petrochronology, Funeral Mountains, California, in Craddock, J.P., Malone, D.H., Foreman, B.Z., and Konstantinou, A. eds., Tectonic Evolution of the Sevier-Laramide Hinterland, Thrust Belt, Foreland and Post-Orogenic Slab Rollback (150-20 Ma), Boulder, Colorado, Geological Society of America.

Anders, M.H., and Sleep, N.H., 1992, Magmatism and extension—The thermal and mechanical effects of the Yellowstone hotspot: Journal of Geophysical Research, v. 97, p. 15,379-15,393, doi:10.1029/92JB01376.

Armstrong, R.L., 1972, Low-angle (denudation) faults, hinterland of the sevier orogenic belt, eastern Nevada and western Utah: Bulletin of the Geological Society of America, v. 83, p. 1729–1754, doi:10.1130/0016-7606(1972)83[1729:LDFHOT]2.0.CO;2.

Armstrong, R.L., 1968, Sevier orogenic belt in Nevada and Utah: Bulletin of the Geological Society of America, v. 79, p. 429–458, doi:10.1130/0016-7606(1968)79[429:SOBINA]2.0.CO;2.

Armstrong, R.L., and Ward, P., 1991, Evolving geographic patterns of Cenozoic magmatism in the North American Cordillera: The temporal and spatial association of magmatism and metamorphic core complexes: Journal of Geophysical Research, v. 96, p. 13,201–13,224, doi:10.1029/91JB00412.

Atwater, T., 1989, Plate tectonic history of the northeast Pacific and western North America, *in* Winterer, E.L., Hussong, D.M., and Decker, R.W. eds., The Geology of North America: The Eastern Pacific Ocean and Hawaii, v. N, p. 499–522.

Atwater, T., and Stock, J.M., 1998, Pacific-North America plate tectonics of the Neogene southwestern United States: An update: International Geology Review, v. 40, p. 375–402, doi:10.1080/00206819809465216.

Axelrod, D.I., 1966, The Eocene Copper Basin flora of northeastern Nevada: Berkeley, University of California Press, v. 59, 83 p.

883 Bahadori, A., and Holt, W.E., 2019, Geodynamic evolution of southwestern North America since
884 the late Eocene: Nature Communications, v. 10, p. 1–18, doi:10.1038/s41467-019-12950-8.
885 Bahadori, A., Holt, W.E., and Rasbury, E.T., 2018, Reconstruction modeling of crustal thickness
886 and paleotopography of western North America since 36 Ma: Geosphere, v. 14, p. 1207–
887 1231, doi:10.1130/GES01604.1.
888 Beranek, L.P., Link, P.K., and Fanning, C.M., 2006, Miocene to Holocene landscape evolution of
889 the western Snake River Plain region, Idaho: Using the SHRIMP detrital zircon provenance
890 record to track eastward migration of the Yellowstone hotspot: Bulletin of the Geological
891 Society of America, v. 118, p. 1027–1050, doi:10.1130/B25896.1.
892 Best, M.G., Barr, D.L., Christiansen, E.H., Gromme, S., Deino, A.L., and Tingey, D.G., 2009,
893 The Great Basin Altiplano during the middle Cenozoic ignimbrite flareup: insights from
894 volcanic rocks: International Geology Review, v. 51, p. 589–633,
895 doi:10.1080/00206810902867690.
896 Best, M.G., and Christiansen, E.H., 1991, Limited extension during peak Tertiary volcanism,
897 Great Basin of Nevada and Utah: Journal of Geophysical Research, v. 96, p. 13509,
898 doi:10.1029/91JB00244.
899 Best, M.G., Christiansen, E.H., and Gromme, S., 2013, Introduction: The 36-18 Ma southern
900 Great Basin, USA, ignimbrite province and flareup: Swarms of subduction-related
901 supervolcanoes: Geosphere, v. 9, p. 260–274, doi:10.1130/GES00870.1.
902 Du Bray, E.A., 2007, Time, space, and composition relations among northern Nevada intrusive
903 rocks and their metallogenic implications: Geosphere, v. 3, p. 381–405,
904 doi:10.1130/GES00109.1.
905 Brooks, W.E., Thorman, C.H., Snee, L.W., and Al, B.E.T., 1995, Ar ages and tectonic setting of
906 the middle Eocene northeast Nevada volcanic field: Journal of Geophysical Research, v.
907 100, p. 10403–10416, doi:10.1029/94JB03389.
908 Van Buer, N.J., and Miller, E.L., 2010, Sahwave batholith, NW Nevada: Cretaceous arc flareup
909 in a basinal terrane: Lithosphere, v. 2, p. 423–446, doi:10.1130/L105.1.
910 Van Buer, N.J., Miller, E.L., and Dumitru, T.A., 2009, Early Tertiary paleogeologic map of the
911 northern Sierra Nevada batholith and the northwestern Basin and Range: Geology, v. 37, p.
912 371–374, doi:10.1130/G25448A.1.
913 Burchfiel, C., Cowan, D.S., and Davis, G.A., 1992, Tectonic overview of the Cordilleran orogen

914 in the western United States, *in* Burchfiel, B.C., Lipman, P.W., and Zoback, M.L. eds., The
915 Geology of North America, v. G-3, p. 407–479.
916 Camilleri, P.A., Deibert, J., and Perkins, M.E., 2017, Middle Miocene to Holocene tectonics,
917 basin evolution, and paleogeography along the southern margin of the Snake River Plain in
918 the Knoll Mountain-Ruby-East Humboldt Range region, northeastern Nevada and south-
919 central Idaho: Geosphere, v. 13, p. 1901–1948, doi:10.1130/GES01318.1.
920 Canada, A.S., Cassel, E.J., Stockli, D.F., Smith, M.E., Jicha, B.R., and Singer, B.S., 2020,
921 Accelerating exhumation in the Eocene North American Cordilleran hinterland:
922 Implications from detrital zircon (U-Th)/(He-Pb) double dating: GSA Bulletin, v. 132, p.
923 198–214, doi:10.1130/B35160.1.
924 Carroll, A.R., Doebbert, A.C., Booth, A.L., Chamberlain, C.P., Rhodes-Carson, M.K., Smith,
925 M.E., Johnson, C.M., and Beard, B.L., 2008, Capture of high-altitude precipitation by a
926 low-altitude Eocene lake, western U.S: Geology, v. 36, p. 791–794,
927 doi:10.1130/G24783A.1.
928 Cassel, E.J., Breecker, D.O., Henry, C.D., Larson, T.E., and Stockli, D.F., 2014, Profile of a
929 paleo-orogen: High topography across the present-day Basin and Range from 40 to 23 Ma:
930 Geology, v. 42, p. 1007–1010, doi:10.1130/G35924.1.
931 Cassel, E.J., Graham, S.A., and Chamberlain, C.P., 2009, Cenozoic tectonic and topographic
932 evolution of the northern Sierra Nevada, California, through stable isotope paleoaltimetry in
933 volcanic glass: Geology, v. 37, p. 547–550, doi:10.1130/G25572A.1.
934 Cassel, E.J., Graham, S.A., Chamberlain, C.P., and Henry, C.D., 2012, Early Cenozoic
935 topography, morphology, and tectonics of the northern Sierra Nevada and western Basin and
936 Range: Geosphere, v. 8, p. 229–249, doi:10.1130/GES00671.1.
937 Cassel, E.J., Smith, M.E., and Jicha, B.R., 2018, The impact of slab rollback on Earth's surface:
938 Uplift and extension in the hinterland of the North American Cordillera: Geophysical
939 Research Letters, p. 1–9, doi:10.1029/2018GL079887.
940 Chamberlain, C.P., Mix, H.T., Mulch, A., Hren, M.T., Kent-Corson, M.L., Davis, S.J., Horton,
941 T.W., and Graham, S.A., 2012, The Cenozoic climatic and topographic evolution of the
942 western North American Cordillera: American Journal of Science, v. 312, p. 213–262,
943 doi:10.2475/02.2012.05.
944 Chamberlain, C.P., Mulch, A., Kent-Corson, M.L., Davis, S.J., Carroll, A.R., and Graham, S.A.,

2007, Cenozoic topographic evolution of the Western North America Cordillera: Geochimica Et Cosmochimica Acta, v. 71, p. A157–A157.

Chase, C.G., Gregory-Wodzicki, K., Parrish, J.T., and DeCelles, P.G., 1998, Topographic history of the Western Cordillera of North America and controls on climate, *in* Crowley, T.J. and Burke, K. eds., Tectonic boundary conditions for climate reconstructions, Oxford University Press, v. 39, p. 73–99, https://books.google.ch/books?hl=en&lr=&id=HbamVUkDTLMC&oi=fnd&pg=PA73&dq=chase+1998+western+cordillera&ots=qen7llUxn_&sig=WUIfZKMs-fTiRgSKQKshUJ8wYUk#v=onepage&q=chase 1998 western cordillera&f=false.

Christiansen, R.L., and Yeats, R.S., 1992, Post-Laramide geology of the US Cordilleran region, *in* Burchfiel, B.C., Lipman, P.W., and Zoback, M.L. eds., The Geology of North America, v. 3, p. 261–406.

Coble, M.A., and Mahood, G.A., 2012, Initial impingement of the Yellowstone plume located by widespread silicic volcanism contemporaneous with Columbia River flood basalts: Geology, v. 40, p. 655–658, doi:10.1130/G32692.1.

Coble, M.A., and Mahood, G.A., 2016, Geology of the High Rock caldera complex, northwest Nevada, and implications for intense rhyolitic volcanism associated with flood basalt magmatism and the initiation of the Snake River Plain- Yellowstone trend: Geosphere, v. 12, p. 58–113, doi:10.1130/GES01162.1.

Colgan, J.P., 2013, Reappraisal of the relationship between the northern Nevada rift and Miocene extension in the northern Basin and Range Province: Geology, v. 41, p. 211–214, doi:10.1130/G33512.1.

Colgan, J.P., Dumitru, T.A., McWilliams, M.O., and Miller, E.L., 2006, Timing of Cenozoic volcanism and Basin and Range extension in northwestern Nevada: New constraints from the northern Pine Forest Range: Bulletin of the Geological Society of America, v. 118, p. 126–139, doi:10.1130/B25681.1.

Colgan, J.P., Dumitru, T.A., and Miller, E.L., 2004, Diachroneity of Basin and Range extension and Yellowstone hotspot volcanism in northwestern Nevada: Geology, v. 32, p. 121, doi:10.1130/G20037.1.

Colgan, J.P., and Henry, C.D., 2009, Rapid middle Miocene collapse of the Mesozoic orogenic plateau in north-central Nevada: International Geology Review, v. 51, p. 920–961,

doi:10.1080/00206810903056731.
Colgan, J.P., and Henry, C.D., 2017, Eruptive history, geochronology, and post-eruption structural evolution of the late Eocene Hall Creek caldera, Toiyabe Range, Nevada: U.S. Geological Survey Professional Paper 1832, 44 p., doi:10.1130/abs/2016am-285314.
Colgan, J.P., Howard, K.A., Fleck, R.J., and Wooden, J.L.P., 2010, Rapid middle Miocene extension and unroofing of the southern Ruby Mountains, Nevada: Tectonics, v. 29, p. 417, doi:10.1029/2009TC002655.
Colgan, J.P., John, D.A., Henry, C.D., and Fleck, R.J., 2008, Large-magnitude Miocene extension of the Eocene Caetano caldera, Shoshone and Toiyabe Ranges, Nevada: Geosphere, v. 4, p. 107–130, doi:10.1130/GES00115.1.
Coney, P.J., and Harms, T.A., 1984, Cordilleran metamorphic core complexes: Cenozoic extensional relics of Mesozoic compression: Geology, v. 12, p. 550–554, doi:10.1130/0091-7613(1984)12<550:CMCCCE>2.0.CO;2.
Cooper, F.J., Platt, J.P., Anczkiewicz, R., and Whitehouse, M.J., 2010, Footwall dip of a core complex detachment fault: Thermobarometric constraints from the northern Snake Range (Basin and Range, USA): Journal of Metamorphic Geology, v. 28, p. 997–1020, doi:10.1111/j.1525-1314.2010.00907.x.
Copeland, P., Currie, C.A., Lawton, T.F., and Murphy, M.A., 2017, Location, location, location: The variable lifespan of the laramide orogeny: Geology, v. 45, p. 223–226, doi:10.1130/G38810.1.
Craddock, J.P., Malone, D.H., Konstantinou, A., Spruell, J., and Porter, R., 2021, Calcite twinning strains associated with Laramide uplifts, Wyoming Province, in Craddock, J.P., Malone, D.H., Foreman, B.Z., and Konstantinou, A. eds., Tectonic Evolution of the Sevier-Laramide Hinterland, Thrust Belt, Foreland and Post-Orogenic Slab Rollback (150-20 Ma), Boulder, Colorado, Geological Society of America.
Crafford, A.E.J., 2007, Geologic Map of Nevada: U.S. Geological Survey Data Series 249: U.S. Geological Survey Data Series 249, p. 46.
Crafford, A.E.J., and Harris, A.G., 2005, New digital conodont color alteration index (CAI) maps of Nevada, *in* Geological Society of America Abstracts with Programs, Salt Lake City, Utah, v. 37, p. 379, https://gsa.confex.com/gsa/2005AM/finalprogram/abstract_94308.htm.
Crough, S.T., 1978, Thermal origin of mid-plate hot-spot swells: Geophysical Journal of the

Royal Astronomical Society, v. 55, p. 451–469, doi:10.1111/j.1365-246X.1978.tb04282.x.
Dallmeyer, R.D., Snoke, A.W., and McKee, E.H., 1986, The Mesozoic-Cenozoic tectonothermal evolution of the Ruby Mountains, East Humboldt Range, Nevada: A Cordilleran metamorphic core complex: Tectonics, v. 5, p. 931, doi:10.1029/TC005i006p00931.
Davis, S.J., Mix, H.T., Wiegand, B.A., Carroll, A.R., and Chamberlain, C.P., 2009, Synorogenic evolution of large-scale drainage patterns: Isotope paleohydrology of sequential laramide basins: American Journal of Science, v. 309, p. 549–602, doi:10.2475/07.2009.02.
Davis, S.J., Mulch, A., Carroll, A.R., Horton, T.W., and Chamberlain, C.P., 2006, Paleogene landscape evolution of the central North American Cordillera: Developing topography and hydrology in the Laramide foreland: Geological Society of America Bulletin, v. preprint, p. 1, doi:10.1130/B26308.1.
DeCelles, P.G., 2004, Late Jurassic to Eocene evolution of the Cordilleran thrust belt and foreland basin system, western U.S.A.: American Journal of Science, v. 304, p. 105–168, doi:10.2475/ajs.304.2.105.
DeCelles, P.G., and Coogan, J.C., 2006, Regional structure and kinematic history of the Sevier fold-and-thrust belt, central Utah: Bulletin of the Geological Society of America, v. 118, p. 841–864, doi:10.1130/B25759.1.
Di Fiori, R.V., Long, S.P., Fetrow, A.C., Snell, K.E., Bonde, J.W., and Vervoort, J., 2020, Syncontractional deposition of the Cretaceous Newark Canyon Formation, Diamond Mountains, Nevada: Implications for strain partitioning within the U.S. Cordillera: Geosphere, v. 16, p. 546–566, doi:10.1130/GES02168.1.
Dickinson, W.R., 2013, Phanerozoic palinspastic reconstructions of Great Basin geotectonics (Nevada-Utah, USA): Geosphere, v. 9, p. 1384–1396, doi:10.1130/GES00888.1.
Dickinson, W.R., and Snyder, W.S., 1978, Plate tectonics of the Laramide orogeny, *in* Geological Society of America Memoir, v. 151, p. 355–366, doi:10.1130/MEM151-p355.
Dokka, R.K., Mahaffie, M.J., and Snoke, A.W., 1986, Thermochronologic evidence of major tectonic denudation associated with detachment faulting, Northern Ruby Mountains-East Humboldt Range, Nevada: Tectonics, v. 5, p. 995, doi:10.1029/TC005i007p00995.
Druschke, P., Hanson, A.D., and Wells, M.L., 2009a, Structural, stratigraphic, and geochronologic evidence for extension predating Palaeogene volcanism in the Sevier hinterland, east-central Nevada: International Geology Review, v. 51, p. 743–775,

doi:10.1080/00206810902917941.
Druschke, P., Hanson, A.D., Wells, M.L., Gehrels, G.E., and Stockli, D.F., 2011, Paleogeographic isolation of the Cretaceous to Eocene Sevier hinterland, east-central Nevada: Insights from U-Pb and (U-Th)/He detrital zircon ages of hinterland strata: Bulletin of the Geological Society of America, v. 123, p. 1141–1160, doi:10.1130/B30029.1.
Druschke, P., Hanson, A.D., Wells, M.L., Rasbury, T., Stockli, D.F., and Gehrels, G.E., 2009b, Synconvergent surface-breaking normal faults of Late Cretaceous age within the Sevier hinterland, east-central Nevada: Geology, v. 37, p. 447–450, doi:10.1130/G25546A.1.
Dubiel, R.F., Potter, C.J., Good, S.C., and Snee, L.W., 1996, Reconstructing an Eocene extensional basin: The White Sage Formation, eastern Great Basin: GSA Special Paper 303, p. 14, doi:10.1130/0-8137-2303-5.1.
Dumitru, T.A., Elder, W.P., Hourigan, J.K., Chapman, A.D., Graham, S.A., and Wakabayashi, J., 2016, Four Cordilleran paleorivers that connected Sevier thrust zones in Idaho to depocenters in California, Washington, Wyoming, and, indirectly, Alaska: Geology, v. 44, p. 75–78, doi:10.1130/G37286.1.
Dumitru, T.A., Ernst, W.G., Hourigan, J.K., and McLaughlin, R.J., 2015, Detrital zircon U–Pb reconnaissance of the Franciscan subduction complex in northwestern California: International Geology Review, v. 57, p. 767–800, doi:10.1080/00206814.2015.1008060.
Fouch, T.D., Hanley, J.H., and Forester, R.M., 1979, Preliminary correlation of Cretaceous and Paleogene lacustrine and related nonmarine sedimentary and volcanic rocks in parts of the eastern Great Basin of Nevada and Utah, *in* 1979 Basin and Range Symposium, Rocky Mountain Association of Geologists, v. 69, p. 305–312.
Frerichs, W.E., and Pekarek, A.H., 1994, Lower Miocene petroleum potential of northeast Elko County, *in* Schalla, R.A. and Johnson, E.H. eds., Oil fields of the Great Basin: Special Publication of the Nevada Petroleum Society, p. 151–159.
Gans, P.B., 1987, An open-system, two-layer crustal stretching model for the eastern Great Basin: Tectonics, v. 6, p. 1–12, doi:10.1029/TC006i001p00001.
Gans, P.B., 1990, Space-time patterns of Cenozoic N–S extension, N–S shortening, E–W extension, and magmatism in the Basin and Range Province: Evidence for active rifting, *in* Geological Society of America Abstracts with Programs, v. 22, p. 24.
Gans, P.B., Mahood, G.A., and Schermer, E., 1989, Synextensional magmatism in the Basin and

Range Province; a case study from the eastern Great Basin: GSA Special Paper 233, p. 1–53, doi:10.1130/SPE233-p1.

Gans, P.B., and Miller, E.L., 1983, Style of mid-Tertiary extension in east-central Nevada: Special Studies of the Utah Geological and Mineral Survey, v. 59, p. 107–160.

Gans, P.B., Repetski, J.E., Harris, A.G., and Clark, D.H., 1990, Conodont geothermometry of Paleozoic supracrustal rocks in the eastern Great Basin, *in* Geological Society of Nevada Symposium, p. 103.

Garside, L.J., Henry, C.D., Faulds, J.E., and Hinz, N.H., 2005, The upper reaches of the Sierra Nevada auriferous gold channels, California and Nevada: Geological Society of Nevada Symposium, p. 209–235.

Gerya, T., 2015, Tectonic overpressure and underpressure in lithospheric tectonics and metamorphism: Journal of Metamorphic Geology, v. 33, p. 785–800, doi:10.1111/jmg.12144.

Goldstrand, P.M., 1992, Evolution of Late Cretaceous and early Tertiary Basins of southwest Utah based on clastic petrology: Journal of Sedimentary Research, v. 62, p. 495–507, doi:10.1306/D4267933-2B26-11D7-8648000102C1865D.

Goldstrand, P.M., 1994, Tectonic development of Upper Cretaceous to Eocene strata of southwestern Utah: Bulletin of the Geological Society of America, v. 106, p. 145–154, doi:10.1130/0016-7606(1994)106<0145.

Gottlieb, E.S., 2018, Geologic insights from zircon inheritance: Stanford University, 354 p.

Gottlieb, E.S., Miller, E.L., Valley, J.W., Premo, W.R., Fisher, C.M., Vervoort, J.D., and Kitajima, K., 2021, Zircon petrochronology of Cretaceous Cordilleran Interior granites in the Sevier hinterland, Nevada, Utah, USA, in Craddock, J.P., Malone, D.H., Foreman, B.Z., and Konstantinou, A. eds., Tectonic Evolution of the Sevier-Laramide Hinterland, Thrust Belt, Foreland and Post-Orogenic Slab Rollback (150-20 Ma), Boulder, Colorado, Geological Society of America.

Haines, S.H., and Van Der Pluijm, B.A., 2010, Dating the detachment fault system of the Ruby Mountains, Nevada: Significance for the kinematics of low-angle normal faults: Tectonics, v. 29, p. TC4028, doi:10.1029/2009TC002552.

Hallett, B.W., and Spear, F.S., 2013, The P-T history of anatectic pelites of the northern East Humboldt Range, Nevada: Evidence for tectonic loading, decompression, and anatexis:

Journal of Petrology, v. 55, p. 3–36, doi:10.1093/petrology/egt057.
Harris, A.G., Wardlaw, B.R., Rust, C.C., and Merrill, G.K., 1980, Maps for assessing thermal maturity (conodont color alteration index maps) in Ordovician through Triassic rocks in Nevada and Utah and adjacent parts of Idaho and California: U.S. Geological Survey Miscellaneous Investigations Series Map I-1249, 1:2,500,000 scale.
Haynes, S.R., 2003, Development of the Eocene Elko Basin, northeastern Nevada: Implications for paleogeography and regional tectonism: The University of British Columbia, https://circle.ubc.ca/bitstream/id/34598/ubc_2003-0240.pdf.
Henry, C.D., 2008, Ash-flow tuffs and paleovalleys in northeastern Nevada: Implications for Eocene paleogeography and extension in the Sevier hinterland, northern Great Basin: Geosphere, v. 4, p. 1–35, doi:10.1130/GES00122.1.
Henry, C.D., 2018, The Eocene Elko Basin and Elko Formation, NE Nevada: Paleotopographic controls on area, thickness, facies distribution, and petroleum potential: AAPG Annual Convention, v. May 20-23, p. 2857031.
Henry, C.D., Hinz, N.H., Faulds, J.E., Colgan, J.P., John, D.A., Brooks, E.R., Cassel, E.J., Garside, L.J., Davis, D.A., and Castor, S.B., 2012, Eocene-early Miocene paleotopography of the Sierra Nevada-Great Basin-Nevadaplano based on widespread ash-flow tuffs and paleovalleys: Geosphere, v. 8, p. 1–27, doi:10.1130/GES00727.1.
Henry, C.D., Jackson, M.R., Mathewson, D.C., Koehler, S.R., and Moore, S.C., 2015, Eocene igneous geology and relation to mineralization: Railroad District, southern Carlin Trend, Nevada, *in* Pennell, W.M. and Garside, L.J. eds., Geological Society of Nevada, New Concepts and Discoveries, p. 939–965.
Henry, C.D., and John, D.A., 2013, Magmatism, ash-flow tuffs, and calderas of the ignimbrite flareup in the western Nevada volcanic field, Great Basin, USA: Geosphere, v. 9, p. 951, doi:10.1130/GES00867.1.
Henry, C.D., McGrew, A.J., Colgan, J.P., Snoke, A.W., and Brueseke, M.E., 2011, Timing, distribution, amount, and style of Cenozoic extension in the northern Great Basin, *in* Evans, J.P. and Lee, J. eds., Geological Society of America Field Guide 21, p. 27–66, doi:10.1130/2011.0021(02).
Henry, C.D., Zuza, A. V., Thorman, C.H., Ressel, M.W., and Dee, S., 2018, Geologic mapping of the Pequop Mountains, NE Nevada: Exploring basic and applied topics in the easternmost

Ruby Mountains-East Humboldt Range metamorphic core complex, *in* AGU Fall Meeting Abstracts,.

Hodges, K. V., Snoke, A.W., and Hurlow, H.A., 1992, Thermal evolution of a portion of the Sevier Hinterland: The Northern Ruby Mountains-East Humboldt Range and Wood Hills, northeastern Nevada: Tectonics, v. 11, p. 154, doi:10.1029/91TC01879.

Hoiland, C.W., Hourigan, J.K., and Miller, E.L., 2021, Evidence for large departures from lithostatic pressure during Late Cretaceous metamorphism in the northern Snake Range metamorphic core complex, Nevada, *in* Craddock, J.P., Malone, D.H., Foreman, B.Z., and Konstantinou, A. eds., Tectonic Evolution of the Sevier-Laramide Hinterland, Thrust Belt, Foreland and Post-Orogenic Slab Rollback (150-20 Ma), Boulder, Colorado, Geological Society of America.

Hollingsworth, E.R., Ressel, M.W., and Henry, C.D., 2017, Age and depth of Carlin-type gold deposits in the southern Carlin trend: Eocene mountain lakes, big volcanoes, and widespread, shallow hydrothermal circulation, *in* Bedell, R.L. and Ressel, M.W. eds., Geological Society of Nevada field trip guidebook: Shallow expressions of Carlin-type gold deposits: Alligator Ridge and Emigrant mines, Nevada, Reno, NV, p. 149–173.

Horton, B.K., and Schmitt, J.G., 1998, Development and exhumation of a Neogene sedimentary basin during extension, east-central Nevada: Bulletin of the Geological Society of America, v. 110, p. 163–172, doi:10.1130/0016-7606(1998)110<0163:DAEOAN>2.3.CO;2.

Horton, T.W., Sjostrom, D.J., Abruzzese, M.J., Poage, M.A., Waldbauer, J.R., Hren, M.T., Wooden, J.L.P., and Chamberlain, C.P., 2004, Spatial and temporal variation of Cenozoic surface elevation in the Great Basin and Sierra Nevada: American Journal of Science, v. 304, p. 862–888, doi:10.2475/ajs.304.10.862.

Howard, K.A., 2003, Crustal structure in the Elko-Carlin Region, Nevada, during Eocene gold mineralization: Ruby-East Humboldt metamorphic core complex as a guide to the deep crust: Economic Geology, v. 98, p. 249–268, doi:10.2113/gsecongeo.98.2.249.

Howard, K.A., Wooden, J.L., Barnes, C.G., Premo, W.R., Snoke, A.W., and Lee, S., 2011, Episodic growth of a Late Cretaceous and Paleogene intrusive complex of pegmatitic leucogranite, Ruby Mountains core complex, Nevada, USA: Geosphere, v. 7, p. 1220, doi:10.1130/GES00668.1.

Humphreys, E.D., 1995, Post-Laramide removal of the Farallon slab, western United States:

Geology, v. 23, p. 987, doi:10.1130/0091-7613(1995)023<0987:PLROTF>2.3.CO;2.
Kent-Corson, M.L., Mulch, A., Graham, S.A., Carroll, A.R., Ritts, B.D., and Chamberlain, C.P., 2010, Diachronous isotopic and sedimentary responses to topographic change as indicators of mid-Eocene hydrologic reorganization in the western United States: Basin Research, v. 22, p. 829–845, doi:10.1111/j.1365-2117.2009.00456.x.
Kent-Corson, M.L., Sherman, L.S., Mulch, A., and Chamberlain, C.P., 2006, Cenozoic topographic and climatic response to changing tectonic boundary conditions in western North America: Earth and Planetary Science Letters, v. 252, p. 453–466, doi:10.1016/j.epsl.2006.09.049.
Ketner, K.B., and Alpha, A.G., 1992, Mesozoic and Tertiary rocks near Elko, Nevada: Evidence for Jurassic to Eocene folding and low-angle faulting: Evolution of sedimentary basins—Eastern Great Basin: U.S. Geological Survey Bulletin 1988-C, p. 13.
Konstantinou, A., 2021, The "death" of the Sevier-Laramide orogen: Gravitational collapse of the crust or something else?, *in* Craddock, J.P., Malone, D.H., Foreman, B.Z., and Konstantinou, A. eds., Tectonic Evolution of the Sevier-Laramide Hinterland, Thrust Belt, Foreland and Post-Orogenic Slab Rollback (150-20 Ma), Boulder, Colorado, Geological Society of America.
Konstantinou, A., and Miller, E.L., 2015, Evidence for a long-lived accommodation/transfer zone beneath the Snake River Plain: A possible influence on Neogene magmatism? Tectonics, v. 34, p. 2387–2398, doi:10.1002/2015TC003863.
Konstantinou, A., Strickland, A., Miller, E.L., Vervoort, J.D., Fisher, C.M., Wooden, J.L.P., and Valley, J.W., 2013a, Synextensional magmatism leading to crustal flow in the Albion-Raft River-Grouse Creek metamorphic core complex, northeastern Basin and Range: Tectonics, v. 32, p. 1384–1403, doi:10.1002/tect.20085.
Konstantinou, A., Strickland, A., Miller, E.L., and Wooden, J.P., 2012, Multistage Cenozoic extension of the Albion–Raft River–Grouse Creek metamorphic core complex: Geochronologic and stratigraphic constraints: Geosphere, v. 8, p. 1429–1466, doi:10.1130/GES00778.1.
Konstantinou, A., Valley, J.W., Strickland, A., Miller, E.L., Fisher, C.M., Vervoort, J.D., and Wooden, J.L.P., 2013b, Geochemistry and geochronology of the Jim Sage volcanic suite, southern Idaho: Implications for Snake River Plain magmatism and its role in the history of

Basin and Range extension: Geosphere, v. 9, p. 1681–1703, doi:10.1130/GES00948.1.
Kreemer, C., Blewitt, G., and Hammond, W.C., 2010, Evidence for an active shear zone in southern Nevada linking the Wasatch fault to the Eastern California shear zone: Geology, v. 38, p. 475–478, doi:10.1130/G30477.1.
Lachenbruch, A.H., and Morgan, P., 1990, Continental extension, magmatism and elevation; formal relations and rules of thumb: Tectonophysics, v. 174, p. 39–62.
Larimer, J.E., Yanites, B.J., Phillips, W., and Mittelstaedt, E., 2019, Late Miocene rejuvenation of central Idaho landscape evolution: A case for surface processes driven by plume-lithosphere interaction: Lithosphere, v. 11, p. 59–72, doi:10.1130/L746.1.
Lechler, A.R., and Niemi, N.A., 2011, Sedimentologic and isotopic constraints on the Paleogene paleogeography and paleotopography of the southern Sierra Nevada, California: Geology, v. 39, p. 379–382, doi:10.1130/G31535.1.
Lechler, A.R., Niemi, N.A., Hren, M.T., and Lohmann, K.C., 2013, Paleoelevation estimates for the northern and central proto-Basin and Range from carbonate clumped isotope thermometry: Tectonics, v. 32, p. 295–316, doi:10.1002/tect.20016.
Lee, J., Blackburn, T., and Johnston, S., 2017, Timing of mid-crustal ductile extension in the northern Snake Range metamorphic core complex, Nevada: Evidence from U/Pb zircon ages: Geosphere, v. 13, p. 439–459, doi:10.1130/GES01429.1.
Lerch, D.W., Miller, E.L., McWilliams, M.O., and Colgan, J.P., 2008, Tectonic and magmatic evolution of the northwestern Basin and Range and its transition to unextended volcanic plateaus: Black Rock Range, Nevada: Bulletin of the Geological Society of America, v. 120, p. 300–311, doi:10.1130/B26151.1.
Levander, A., and Miller, M.S., 2012, Evolutionary aspects of lithosphere discontinuity structure in the western U.S.: Geochemistry, Geophysics, Geosystems, v. 13, p. n/a-n/a, doi:10.1029/2012GC004056.
Lewis, C.J., Wernicke, B.P., Selverstone, J., and Bartley, J.M., 1999, Deep burial of the footwall of the northern Snake Range decollement, Nevada: Bulletin of the Geological Society of America, v. 111, p. 39–51, doi:10.1130/0016-7606(1999)111<0039:DBOTFO>2.3.CO;2.
Liu, L., and Stegman, D.R., 2012, Origin of Columbia River flood basalt controlled by propagating rupture of the Farallon slab: Nature, v. 482, p. 386–389, doi:10.1038/nature10749.

Lofgren, D.L., Honey, J.G., McKenna, M.C., Zondervan, R.L., and Smith, E.E., 2008, Paleocene primates from the Goler Formation of the Mojave Desert in California, *in* Wang, X. and Barnes, L.G. eds., Science Series 41: Geology and Vertebrate Paleontology of Western and Southern North America, Natural History Museum of Los Angeles County, p. 11–28.

Long, S.P., 2018, Geometry and extension magnitude of the Basin and Range Province (39°N), Utah, Nevada, and California, USA: Constraints from a province-scale cross section: Geological Society of America Bulletin, doi:10.1130/B31974.

Long, S.P., 2012, Magnitudes and spatial patterns of erosional exhumation in the Sevier hinterland, eastern Nevada and western Utah, USA: Insights from a Paleogene paleogeologic map: Geosphere, v. 8, p. 881, doi:10.1130/GES00783.1.

Lund, K., 2008, Geometry of the Neoproterozoic and Paleozoic rift margin of western Laurentia: Implications for mineral deposit settings: Geosphere, v. 4, p. 429, doi:10.1130/GES00121.1.

Lund, K., Beard, L.S., and Perry, W.J., 1993, Relation between extensional geometry of the northern Grant Range and oil occurrences in Railroad Valley, east-central Nevada: AAPG Bulletin, v. 77, p. 945–962.

Lund Snee, J.-E., 2013, Geology and geochronology of Cenozoic units in the Piñon Range and Huntington Valley, Nevada: Stanford University, 263 p., http://purl.stanford.edu/hx388mg6634.

Lund Snee, J.-E., and Miller, E.L., 2015, Preliminary geologic map of Cenozoic units of the central Robinson Mountain volcanic field and northwestern Huntington Valley: Nevada Bureau of Mines and Geology Open File, v. 15–2, p. 42, 1:24,000 scale, http://pubs.nbmg.unr.edu/product-p/of2015-02.htm.

Lund Snee, J.-E., Miller, E.L., Grove, M., Hourigan, J.K.J.K., and Konstantinou, A., 2016, Cenozoic paleogeographic evolution of the Elko Basin and surrounding region, northeast Nevada: Geosphere, v. 12, p. 464–500, doi:10.1130/GES01198.1.

MacCready, T., Snoke, A.W., Wright, J.E., and Howard, K. a., 1997, Mid-crustal flow during Tertiary extension in the Ruby Mountains core complex, Nevada: Bulletin of the Geological Society of America, v. 109, p. 1576–1594, doi:10.1130/0016-7606(1997)109<1576:MCFDTE>2.3.CO;2.

MacGinitie, H.D., 1941, Contributions to Paleontology: Middle Eocene flora from the central Sierra Nevada: Washington, D.C., Carnegie Institution of Washington Publication 534.

McCrory, P.A., Blair, J.L., Waldhauser, F., and Oppenheimer, D.H., 2012, Juan de Fuca slab geometry and its relation to Wadati-Benioff zone seismicity: Journal of Geophysical Research: Solid Earth, v. 117, doi:10.1029/2012JB009407.

McGrew, A.J., Foland, K.A., and Stockli, D.F., 2007, Evolution of Cenozoic volcanism and extension in the Copper Mountains, northeastern Nevada, *in* Abstracts with Programs - Geological Society of America, v. 39, p. 226, http://search.proquest.com/docview/50467319?accountid=14503%5Cnhttp://libraries.colorado.edu:4550/resserv?genre=article&issn=00167592&title=Abstracts+with+Programs+-+Geological+Society+of+America&volume=39&issue=6&date=2007-10-01&atitle=Evolution+of+Cenoz.

McGrew, A.J., Peters, M.T., and Wright, J.E., 2000, Thermobarometric constraints on the tectonothermal evolution of the East Humboldt Range metamorphic core complex, Nevada: Bulletin of the Geological Society of America, v. 112, p. 45–60, doi:10.1130/0016-7606(2000)112<45:TCOTTE>2.0.CO;2.

McGrew, A.J., and Snee, L.W., 1994, 40Ar/39Ar thermochronologic constraints on the tectonothermal evolution of the northern East Humboldt Range metamorphic core complex, Nevada: Tectonophysics, v. 238, p. 425–450, doi:10.1016/0040-1951(94)90067-1.

McGrew, A.J., and Snoke, A.W., 2015, Geology of the Welcome Quadrangle and adjacent part of the Wells Quadrangle, Elko County, Nevada: Nevada Bureau of Mines and Geology Map 184, 1:24,000 scale, 40 p., 2 sheets.

McQuarrie, N., and Chase, C.G., 2000, Raising the Colorado Plateau: Geology, v. 28, p. 91, doi:10.1130/0091-7613(2000)028<0091:RTCP>2.0.CO;2.

McQuarrie, N., and Wernicke, B.P., 2005, An animated tectonic reconstruction of southwestern North America since 36 Ma: Geosphere, v. 1, p. 147–172, doi:10.1130/GES00016.1.

Malone, D.H., Craddock, J.P., and Konstantinou, A., 2021, Timing and structural evolution of the Sevier thrust belt, *in* Craddock, J.P., Malone, D.H., Foreman, B.Z., and Konstantinou, A. eds., Tectonic Evolution of the Sevier-Laramide Hinterland, Thrust Belt, Foreland and Post-Orogenic Slab Rollback (150-20 Ma), Boulder, Colorado, Geological Society of America.

Miller, E.L., Dumitru, T.A., Brown, R.W., and Gans, P.B., 1999, Rapid Miocene slip on the Snake Range–Deep Creek Range fault system, east-central Nevada: Geological Society of America Bulletin, v. 111, p. 886–905, doi:10.1130/0016-

7606(1999)111<0886:RMSOTS>2.3.CO;2.
Miller, E.L., and Gans, P.B., 1989, Cretaceous crustal structure and metamorphism in the hinterland of the Sevier thrust belt, western U.S. Cordillera: Geology, v. 17, p. 59–62, doi:10.1130/0091-7613(1989)017<0059.
Miller, E.L., Konstantinou, A., and Strickland, A., 2012, Comment on "Geodynamics of synconvergent extension and tectonic mode switching: Constraints from the Sevier-Laramide orogen" by Michael L. Wells et al.: Tectonics, v. 31, p. n/a-n/a, doi:10.1029/2012TC003103.
Miller, E.L., Raftrey, M.E., and Lund Snee, J.-E., 2021, Downhill from Austin and Ely to Las Vegas: U-Pb detrital zircon suites from the Eocene-Oligocene Titus Canyon Formation and associated strata, Death Valley, CA, *in* Craddock, J.P., Malone, D.H., Foreman, B.Z., and Konstantinou, A. eds., Tectonic Evolution of the Sevier-Laramide Hinterland, Thrust Belt, Foreland and Post-Orogenic Slab Rollback (150-20 Ma), Boulder, Colorado, Geological Society of America.
Miller, E.L., Raftrey, M.E., Perez-Lopez, S.A., and Harbaugh, D.W., 2019, Preliminary detrital zircon study of the Oligocene Titus Canyon Formation, Death Valley, suggests central Nevada sources, *in* Geological Society of America Abstracts with Programs. Vol. 51, No. 4, doi:10.1130/abs/2019CD-329243.
Mix, H.T., Mulch, A., Kent-Corson, M.L., and Chamberlain, C.P., 2011, Cenozoic migration of topography in the North American Cordillera: Geology, v. 39, p. 87–90, doi:10.1130/G31450.1.
Moore, S.W., Madrid, H.B., and Server, G.T., 1983, Results of oil-shale investigations in northeastern Nevada: U.S. Geological Survey Open File Report 83-586, p. C1--C18.
Mulch, A., Chamberlain, C.P., Cosca, M.A., Teyssier, C., Methner, K., Hren, M.T., and Graham, S.A., 2015, Rapid change in high-elevation precipitation patterns of western North America during the Middle Eocene Climatic Optimum (MECO): American Journal of Science, v. 315, p. 317–336, doi:10.2475/04.2015.02.
Noble, D.C., 1972, Some observations on the Cenozoic volcano-tectonic evolution of the Great Basin, western United States: Earth and Planetary Science Letters, v. 17, p. 142–150, doi:10.1016/0012-821X(72)90269-5.
Parsons, T., Thompson, G.A., and Sleep, N.H., 1994, Mantle plume influence on the Neogene

uplift and extension of the US western Cordillera? Geology, v. 22, p. 83–86, doi:10.1130/0091-7613(1994)022<0083:MPIOTN>2.3.CO;2.

Pierce, K.L., and Morgan, L.A., 2009, Is the track of the Yellowstone hotspot driven by a deep mantle plume? --- Review of volcanism, faulting, and uplift in light of new data: Journal of Volcanology and Geothermal Research, v. 188, p. 1–25, doi:10.1016/j.jvolgeores.2009.07.009.

Pierce, K.L., Morgan, L.A., and Link, P.K., 1992, The track of the Yellowstone hot spot: Volcanism, faulting, and uplift: Regional geology of eastern Idaho and western Wyoming: Geological Society of America Memoir, v. 179, p. 1–53.

Potter, C.J., Dubiel, R.F., Snee, L.W., and Good, S.C., 1995, Eocene extension of early Eocene lacustrine strata in a complex deformed Sevier-Laramide hinterland, northwest Utah and northeast Nevada: Geology, v. 23, p. 181–184, doi:10.1130/0091-7613(1995)023<0181:EEOEEL>2.3.CO;2.

Rahl, J.M., McGrew, A.J., and Foland, K.A., 2002, Transition from Contraction to Extension in the Northeastern Basin and Range: New Evidence from the Copper Mountains, Nevada: The Journal of Geology, v. 110, p. 179–194, doi:10.1086/338413.

Reid, S.A., 1988, Late Cretaceous and Paleogene sedimentation along east side of San Joaquin Basin, California, *in* Graham, S.A. ed., Studies of the Geology of the San Joaquin Valley, Pacific Section, SEPM (Society for Sedimentary Geology), v. 60, p. 157–171, doi:10.1306/94885890-1704-11D7-8645000102C1865D.

Ressel, M.W., and Henry, C.D., 2006, Igneous geology of the Carlin trend, Nevada: Development of the Eocene plutonic complex and significance for Carlin-type gold deposits: Economic Geology, v. 101, p. 347–383, doi:10.2113/gsecongeo.101.2.347.

Ruksznis, A., 2015, Geology and geochronology of Cenozoic sedimentary basins, east-central Nevada: Stanford University, 219 p.

Ryskamp, E.B., Abbott, J.T., Christiansen, E.H., Keith, J.D., Vervoort, J.D., and Tingey, D.G., 2008, Age and petrogenesis of volcanic and intrusive rocks in the Sulphur Spring Range, central Nevada: Comparisons with ore-associated Eocene magma systems in the Great Basin: Geosphere, v. 4, p. 496, doi:10.1130/GES00113.1.

Saleeby, J.B., Ducea, M.N., Busby, C.J., Nadin, E.S., and Wetmore, P.H., 2008, Chronology of pluton emplacement and regional deformation in the southern Sierra Nevada batholith,

California: Special Paper of the Geological Society of America, v. 438, p. 397–427, doi:10.1130/2008.2438(14).

Satarugsa, P., and Johnson, R.A., 2000, Cenozoic tectonic evolution of the Ruby Mountains metamorphic core complex and adjacent valleys, northeastern Nevada: Rocky Mountain Geology, v. 35, p. 205–230, doi:10.2113/35.2.205.

Schmalholz, S.M., Medvedev, S., Lechmann, S.M., and Podladchikov, Y.Y., 2014, Relationship between tectonic overpressure, deviatoric stress, driving force, isostasy and gravitational potential energy: Geophysical Journal International, p. 680–696, doi:10.1093/gji/ggu040.

Schwartz, T.M., Methner, K., Mulch, A., Graham, S.A., and Chamberlain, C.P., 2019, Paleogene topographic and climatic evolution of the Northern Rocky Mountains from integrated sedimentary and isotopic data: Bulletin of the Geological Society of America, v. 131, p. 1203–1223, doi:10.1130/B32068.1.

Schwartz, T.M., and Schwartz, R.K., 2013, Paleogene postcompressional intermontane basin evolution along the frontal Cordilleran fold-and-thrust belt of southwestern Montana: Bulletin of the Geological Society of America, v. 125, p. 961–984, doi:10.1130/B30766.1.

Server, G.T., and Solomon, B.J., 1983, Geology and oil shale deposits of the Elko Formation, Pinon Range, Elko County, Nevada: U.S. Geological Survey Miscellaneous Field Studies Map MF-1546, 1:24,000 scale.

Sharman, G.R., Graham, S.A., Grove, M., Kimbrough, D.L., and Wright, J.E., 2015, Detrital zircon provenance of the Late Cretaceous-Eocene California forearc: Influence of Laramide low-angle subduction on sediment dispersal and paleogeography: Bulletin of the Geological Society of America, v. 127, p. 38–60, doi:10.1130/B31065.1.

Shen, W., and Ritzwoller, M.H., 2016, Crustal and uppermost mantle structure beneath the United States: Journal of Geophysical Research: Solid Earth, v. 121, p. 4306–4342, doi:10.1002/2016JB012887.

Sluijs, A., Zeebe, R.E., Bijl, P.K., and Bohaty, S.M., 2013, A middle Eocene carbon cycle conundrum: Nature Geoscience, v. 6, p. 429–434, doi:10.1038/ngeo1807.

Smith, M.E., Cassel, E.J., Jicha, B.R., Singer, B.S., and Canada, A.S., 2017, Hinterland drainage closure and lake formation in response to middle Eocene Farallon slab removal, Nevada, U.S.A.: Earth and Planetary Science Letters, v. 479, p. 156–169, doi:10.1016/j.epsl.2017.09.023.

Smith, J.F., and Howard, K.A., 1977, Geologic map of the Lee Quadrangle: U.S. Geological Survey Map GQ-1393, 1:62,500 scale.

Smith, J.F., and Ketner, K.B., 1978, Geologic map of the Carlin-Pinon Range area, Elko and Eureka Counties, Nevada: U.S. Geological Survey Miscellaneous Investigations Series I-1028, 1:62,500 scale.

Smith, J.F., and Ketner, K.B., 1976, Stratigraphy of post-Paleozoic rocks and summary of resources in the Carlin-Pinon Range area, Nevada: U.S. Geological Survey Professional Paper 867-B, p. 1–48.

Smith, D.L., Miller, E.L., Wyld, S.J., and Wright, J.E., 1993, Progression and timing of Mesozoic crustal shortening in the northern Great Basin, western U.S.A, *in* Mesozoic Paleogeography of the Western United States-II, v. 71, p. 389–406, http://archives.datapages.com.stanford.idm.oclc.org/data/pac_sepm/088/088001/pdfs/389.pdf.

Snell, K.E., Koch, P.L., Druschke, P., Foreman, B.Z., and Eiler, J.M., 2014, High elevation of the 'Nevadaplano' during the Late Cretaceous: Earth and Planetary Science Letters, v. 386, p. 52–63, doi:10.1016/j.epsl.2013.10.046.

Solomon, B.J., McKee, E.H., and Andersen, D.W., 1979, Stratigraphy and depositional environments of Paleogene rocks near Elko, Nevada, *in* Pacific Coast Paleogeography Symposium 3: Cenozoic Paleogeography of the Western United States, Pacific Section, SEPM (Society for Sedimentary Geology), p. 75–88.

Sonder, L.J., England, P.C., Wernicke, B.P., and Christiansen, R.L., 1987, A physical model for Cenozoic extension of western North America: Geological Society, London, Special Publications, v. 28, p. 187–201, doi:10.1144/GSL.SP.1987.028.01.14.

Spear, F.S., Thomas, J.B., and Hallett, B.W., 2014, Overstepping the garnet isograd: A comparison of QuiG barometry and thermodynamic modeling: Contributions to Mineralogy and Petrology, v. 168, doi:10.1007/s00410-014-1059-6.

Stewart, J.H., 1980, Geology of Nevada: Nevada Bureau of Mines and Geology, Special Publication, v. 4, p. 136.

Stockli, D.F., 2005, Application of low-temperature thermochronometry to extensional tectonic settings: Reviews in Mineralogy and Geochemistry, v. 58, p. 411–448, doi:10.2138/rmg.2005.58.16.

Stockli, D.F., Surpless, B., Dumitru, T.A., and Farley, K. a., 2002, Thermochronological constraints on the timing and magnitude of Miocene and Pliocene extension in the central Wassuk Range, western Nevada: Tectonics, v. 21, p. 10–19, doi:10.1029/2001TC001295.

Strickland, A., Miller, E.L., Wooden, J.L., Kozdon, R., and Valley, J.W., 2011, Syn-extensional plutonism and peak metamorphism in the Albion-Raft River-Grouse Creek metamorphic core complex: American Journal of Science, v. 311, p. 261–314, doi:10.2475/04.2011.01.

Surpless, B., Stockli, D.F., Dumitru, T.A., and Miller, E.L., 2002, Two-phase westward encroachment of Basin and Range extension into the northern Sierra Nevada: Tectonics, v. 21, p. 2-1-2–13, doi:10.1029/2000TC001257.

Taylor, W.J., Bartley, J.M., Martin, M.W., Geissman, J.W., Walker, J.D., Armstrong, P.A., and Fryxell, J.E., 2000, Relations between hinterland and foreland shortening: Sevier orogeny central North American Cordillera: Tectonics, v. 19, p. 1124–1143, doi:10.1029/1999TC001141.

Thatcher, W., Foulger, G.R., Julian, B.R., Svarc, J., Quilty, E., and Bawden, G.W., 1999, Present-day deformation across the Basin and Range Province, Western United States: Science, v. 283, p. 1714–1717, doi:10.1126/science.283.5408.1714.

Thorman, C.H., Ketner, K.B., Brooks, W.E., Snee, L.W., Zimmerman, R.A., and Raines, G.L., 1991, Late Mesozoic-Cenozoic tectonics in northeastern Nevada, *in* Geology and ore deposits of the Great Basin: Symposium Proceedings, Geological Society of Nevada, Reno, Nevada, v. 1, p. 25–45, doi:10.12681/eadd/1834.

Thorman, C.H., and Peterson, F., 2003, The Middle Jurassic Elko orogeny: A major tectonic event in Nevada-Utah, *in* Annual Meeting Expanded Abstracts, v. 12, p. 169–174.

Thorman, C.H., Sandberg, C.A., Henry, C.D., Zuza, A. V., and Ressel, M.W., 2020, Regional tectonics based on conodont CAIs and burial depths, as viewed from the Pequop Mountains, NE Nevada – An Unbiased Opinion(?), *in* Geological Society of Nevada Symposium: Vision for Discovery: Geology and Ore Deposits of the Basin and Range,.

Tian, Y., and Zhao, D., 2012, P-wave tomography of the western United States: Insight into the Yellowstone hotspot and the Juan de Fuca slab: Physics of the Earth and Planetary Interiors, v. 200–201, p. 72–84, doi:10.1016/j.pepi.2012.04.004.

Tosdal, R.M., Wooden, J.L., and Kistler, R.W., 2000, Geometry of the Neoproterozoic continental break-up, and implications for location of Nevadan mineral belts, *in* Cluer, J.K.,

Price, J.G., Struhsacker, E.M., Hardyman, R.F., and Morris, C.L. eds., Geology and Ore Deposits 2000: The Great Basin and Beyond Proceedings Volume I, p. 451–466.

Vandervoort, D.S., and Schmitt, J.G., 1990, Cretaceous to early Tertiary paleogeography in the hinterland of the Sevier thrust belt, east-central Nevada: Geology, v. 18, p. 567–570, doi:10.1130/0091-7613(1990)018<0567:CTETPI>2.3.CO;2.

Wallace, A.R., Perkins, M.E., and Fleck, R.J., 2008, Late Cenozoic paleogeographic evolution of northeastern Nevada: Evidence from the sedimentary basins: Geosphere, v. 4, p. 36–74, doi:10.1130/GES00114.1.

Wells, M.L., and Hoisch, T.D., 2012, Reply to comment by E. L. Miller et al. on "Geodynamics of synconvergent extension and tectonic mode switching: Constraints from the Sevier-Laramide orogen": Tectonics, v. 31, p. n/a-n/a, doi:10.1029/2012TC003136.

Wells, M.L., Hoisch, T.D., Cruz-Uribe, A.M., and Vervoort, J.D., 2012, Geodynamics of synconvergent extension and tectonic mode switching: Constraints from the Sevier-Laramide orogen: Tectonics, v. 31, p. 1–20, doi:10.1029/2011TC002913.

Willden, R., and Kistler, R.W., 1979, Precambrian and Paleozoic stratigraphy in central Ruby Mountains, Elko County, Nevada, *in* Newman, G.W. and Goode, H.D. eds., Basin and Range Symposium and Great Basin Field Conference, Denver, CO, Rocky Mountain Association of Geologists, p. 221–243.

Willden, R., and Kistler, R.W., 1979, Precambrian and Paleozoic stratigraphy in central Ruby Mountains, Elko County, Nevada, *in* Newman, G.W. and Goode, H.D. eds., Basin and Range Symposium, Denver, CO, Rocky Mountain Association of Geologists, p. 221–243.

Wolfe, J.A., Forest, C.E., and Molnar, P., 1998, Paleobotanical evidence of Eocene and Oligocene paleoaltitudes in midlatitude western North America: Bulletin of the Geological Society of America, v. 110, p. 664–678, doi:10.1130/0016-7606(1998)110<0664:PEOEAO>2.3.CO;2.

Wright, J.E., and Snoke, A.W., 1993, Tertiary magmatism and mylonitization in the Ruby-East Humboldt metamorphic core complex, northeastern Nevada: U-Pb geochronology and Sr, Nd, and Pb isotope geochemistry: Geological Society of America Bulletin, v. 105, p. 935–952, doi:10.1130/0016-7606(1993)105<0935:TMAMIT>2.3.CO;2.

Yeend, W.R., 1974, Gold-bearing gravels of the ancestral Yuba River, Sierra Nevada, California: U.S. Geological Survey Professional Paper 772.

Yonkee, W.A., Dehler, C.D., Link, P.K., Balgord, E.A., Keeley, J.A., Hayes, D.S., Wells, M.L., Fanning, C.M., and Johnston, S.M., 2014, Tectono-stratigraphic framework of Neoproterozoic to Cambrian strata, west-central US: Protracted rifting, glaciation, and evolution of the North American Cordilleran margin: Earth-Science Reviews, v. 136, p. 59–95.

Zachos, J., Pagani, M., Sloan, L., Thomas, E., and Billups, K., 2001, Trends, rhythms, and aberrations in global climate 65 Ma to present: Science, v. 292, p. 686–693, doi:10.1126/science.1059412.

Zuza, A. V, Thorman, C.H., Henry, C.D., Levy, D.A., Dee, S., Long, S.P., Sandberg, C.A., and Soignard, E., 2020, Pulsed Mesozoic deformation in the Cordilleran hinterland and evolution of the Nevadaplano: Insights from the Pequop Mountains, NE Nevada: Lithosphere, v. 1, p. 1–24.